Wireless Pers Commun (2008) 44:423–453
DOI 10.1007/s11277-007-9366-0

Closed-loop Grouped Space–Time Block Code: Encoding, Decoding and Codeword Selection

Chung-Lien Ho · Fan-Shuo Tseng · Ta-Sung Lee

Published online: 12 October 2007

Abstract A design of closed-loop grouped space–time block codes (G-STBCs) including encoding, decoding and codeword selection is proposed for the downlink over Rayleigh flat-fading channels. In particular, at the transmitter, the antenna array is partitioned into a number of groups, each of which is encoded based on the orthogonal STBC (O-STBC). At the receiver, by exploiting the algebraic structure of orthogonal codes, a low-complexity, in recursion form, group-wise ordered successive interference cancellation (OSIC) detector is developed. Moreover, the G-STBC codeword is designed and a G-STBC codeword selection criterion that minimizes the BER performance under the constraints of a fixed spectral efficiency and total transmit power is then proposed. The selection index of the G-STBC codeword and the associated modulation type are determined at the receiver and conveyed to the transmitter with a limited feedback overhead to choose an appropriate mode for transmission. Finally, Numerical examples are used for illustrating the performance of the proposed G-STBCs, OSIC based detection and G-STBC codeword selection criterion.

Keywords Multi-input multi-output (MIMO) · Grouped space–time block code (G-STBC) · Ordered successive interference canceller (OSIC) · Closed-loop

C. -L. Ho
Information and Communications Research Laboratories, New Mobile Access Technology Department, Industrial Technology Research Institute, Chutung, Hsinchu, Taiwan 310, ROC
e-mail: clho@itri.org.tw

F. -S. Tseng (✉) · T. -S. Lee
Department of Communication Engineering and Microelectronics and Information Systems Research Center, National Chiao Tung University, Hsinchu, Taiwan 300, ROC
e-mail: stron.cm93g@nctu.edu.tw

T. -S. Lee
e-mail: tslee@mail.nctu.edu.tw

1 Introduction

Future wireless applications such as the 3GPP long-term evaluation (LTE) [1] and IEEE 802.16e-2005 [2] create the insatiability in the demand for "high data rate" and "high link quality" wireless access [3–5]. Since the communications spectrum is a scarce and very expensive resource, an efficient spectrum management is crucial for achieving the high spectral efficiency. While the conventional temporal, or frequency domain only signal processing techniques would suffer from the need of additional bandwidth, the spatial domain approaches are known to be capable of enhancing signal quality and system capacity through exploiting the spatial resource [6,7]. The adoption of multiple antennas at the transmitter and the receiver, i.e., the multi-input multi-output (MIMO) techniques [8–13], promises a significant increase in data rate and link quality without bandwidth expansion and is thus capable of meeting the formidable service requirements in the next-generation wireless communications.

The core scheme of MIMO systems is the space–time coding (STC) [3–5], [7–14]. The two main functions of STC are spatial multiplexing (SM) and transmit diversity (TD). High spectral efficiency can be achieved through SM by simultaneously transmitting independent data streams from different antennas, e.g., layered STCs (LSTCs) or a.k.a., the Bell Labs layered ST (BLAST) techniques [8–10]. High link quality, on the other hand, is guaranteed if redundant signals are made and sent from different antennas through independent channels to the receiver. The ST block codes (STBCs) [12,13] and ST trellis codes [11] are the two well-known TD techniques in MIMO systems. In particular, these goals may be mutually conflicting, and some compromise is needed to optimize the system performance [7,15]. SM and TD are two extreme and complementary transmission strategies in MIMO systems. In a rich-scattering environment, the SM technique is the most effective solution for achieving high data rate transmission. However, in such an environment, the receive signal-to-noise ratio (SNR) for certain links may be low due to deep channel fades or a large path-loss [7]. The high-rate benefit of SM can thus be largely annihilated by extremely poor detection performance. On the other hand, in the SM scheme, the receiver must have sufficient degrees of freedom to effectively separate the signals transmitted from all transmit antennas. Linear algebra indicates that at least N degrees of freedom is needed to separate N signals. Since the receiver degrees of freedom are offered by the receive antennas, the number of receive antennas must not be smaller than that of transmit antennas, which is an unfavorable factor for mobile terminals. On the contrary, TD scheme is an effective solution, in general suitable for a small-size transmit antenna array (less than four antenna elements), to maintain link robustness over a severely fading environment. Equivalently, a good link quality guarantee achieved by TD can allow high data rate transmission through the use of high order modulation. However, power requirement becomes excessive and hardware realization becomes more complex, leading to a limit in performance [16]. A feasible solution without leveraging the power resource is to combine these two transmission techniques for jointly promoting the data rate and compensating the link loss.

To promote a high-speed transmission with an utmost data transmission efficiency, a prospective approach, therefore, is to look for a certain transmission strategy that can boost as much as possible the data rate for good link channels and, on the other hand, switch to other securing mechanisms for guarding the data from channel impairments if any [17]. To build up such a high-throughput system, we suggest endowing the transmitter with the flexibility in choosing a flexible and robust signal transmission scheme better suited to system requirements and/or channel conditions. Therefore, a more general scheme combining the concepts of SM and TD techniques is considered at the transmitter in this paper. Specifically, we first decouple the transmit antenna array into several groups, with each having the number

of antennas from two to four and being encoded via the orthogonal based ST block codes (O-STBCs) [13]. We refer to the coding scheme as the "grouped STBC (G-STBC)", and the structure of antenna grouping (or antenna group configuration) is called a G-STBC codeword. Such a transmit antenna configuration of a G-STBC codeword can be regarded as a variation of the SM signaling strategy by treating one antenna group as a particular data stream unit (or the so called layer). As a result, the G-STBC can be regarded as a mixed architecture which has the advantages of SM and TD based transmit schemes. Essentially, since multiple code rates can be provided by such an encoding strategy over a block of symbols at the transmitter, it can also be referred to as a "variable-rate" STBC scheme. This coding strategy is different from the scheme proposed in [18], which mainly focuses on a small-size transmit antenna array.

In this paper, a flexible G-STBC scheme with an arbitrary number of transmit antennas is developed for the downlink over Rayleigh flat-fading channels. By adopting the proposed G-STBC encoding strategy, the number of receive antennas used at the user terminal can thus be greatly reduced without performance loss, meeting the practical consideration in implementation cost and physical size. The main motivations of adopting the proposed G-STBC are described in the sequel. Considering that each antenna group is an independent data stream unit, signal detection/interference suppression becomes a factor dominating the link performance in such a system. As known, to detect the transmitted symbols, the optimal solution is the maximum likelihood (ML) detection [7,14]. However, ML is usually prohibitive for practical use due to its high computational complexity. Recently, there are various alternative interference mitigation schemes reported in the literature [19,26]. It was suggested in [24,26] that this problem can be tackled through a multi-user (MU) detection framework, and demonstrated that if all users use O-STBC scheme with the same number of antennas for transmission, then the ordered successive interference cancellation (OSIC) detector would allow a "user-wise" joint detection. By adopting this detection framework, it is shown in this paper that an "antenna group-wise" detection property can be applied to the real-valued constellations in the proposed G-STBC system. However, for complex-valued constellations, it is shown that the per-antenna group detection property will no longer hold leading to extra computational burden. To remedy this, we propose a new OSIC detector for which the antenna group-wise detection property holds for all possible G-STBC codewords be it real or complex. Moreover, a computationally efficient recursion based implementation associated with such an OSIC detector is then developed based on the distinctive structures embedded in the matched-filtered channel matrix (MFCM) [25] to further alleviate the detection computational load. Besides, the codeword structures are studied and a G-STBC codeword selection criterion is proposed based on the minimum BER performance under the fixed total transmit power and total spectral efficiency constraint. As a result, The selected G-STBC codeword and associated modulation scheme can be regarded as a mode, and the selection index of the mode can be conveyed from the receiver to the transmitter with a limited feedback overhead. Finally, numerical examples are given to illustrate the performance of the proposed G-STBCs and corresponding OSIC detector.

2 System Model

2.1 System Description and Basic Assumptions

Consider the G-STBC system over a Rayleigh flat-fading channel as illustrated in Fig. 1, in which N antennas are placed at the transmitter and M antennas are placed at the receiver.

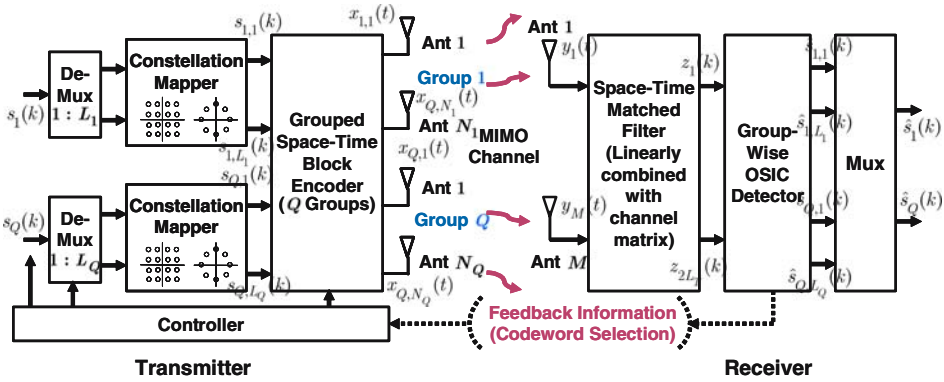

Fig. 1 Transmitter and receiver architectures

The N transmit antenna elements are partitioned into Q antenna groups as $(N_1, \ldots, N_Q)$ with each comprising $2 \le N_q \le 4$ ($\le N$) antennas[1] so that $N_1 + N_2 + \cdots + N_Q = N$. In particular, for the qth group, consecutive B_q symbols of the data stream are spatially and temporally encoded according to O-STBC, and then transmitted across N_q antennas over K_q symbol periods. Assume that unit-rate codes for real-valued constellations with $2 \le N_q \le 4$ and complex-valued constellations with $N_q = 2$, and half-rate codes for complex-valued constellations with $3 \le N_q \le 4$ can be applied to each antenna group. If $K := \max\{K_1, K_2, \ldots, K_Q\}$, then according to the property of O-STBCs, K will be a multiple of K_q, i.e., $K = \kappa_q K_q$ where $\kappa_q := K/K_q$ is a positive integer. During K symbol periods, each antenna group sends $L_q := \kappa_q B_q$ independent symbols, and there are thus in total $L_T := \sum_{q=1}^{Q} L_q = K \sum_{q=1}^{Q} (B_q/K_q)$ data symbols transmitted from the Q antenna groups every K symbol periods. Each antenna group's code, called the *group code*, can be completely described by an associated $N_q \times K$ ST codeword matrix $\mathbf{X}_q(k)$, $q = 1, \ldots, Q$. Dividing the data stream of the qth antenna group $s_q(k)$ into blocks of sub-streams as $s_{q,l}(k) := s_q(L_q k + l - 1)$, $l = 1, \ldots, L_q$, then the ST codeword matrix of the qth group can be written as

$$\mathbf{X}_q(k) := \sum_{l=1}^{2L_q} \mathbf{A}_{q,l} \tilde{s}_{q,l}(k), \tag{1}$$

where $\mathbf{A}_{q,l} \in \mathrm{C}^{N_q \times K}$ is the ST modulation matrix having the following properties:

$$\begin{cases} \mathbf{A}_{q,k}\mathbf{A}_{q,l}^H = \frac{K_q}{N_q P_q}\mathbf{I}_{N_q} & k = l, \\ \mathbf{A}_{q,k}\mathbf{A}_{q,l}^H + \mathbf{A}_{q,l}\mathbf{A}_{q,k}^H = \mathbf{O}_{N_q} & k \ne l. \end{cases} \tag{2}$$

The split real-valued symbols $\tilde{s}_{q,l}(k)$ is defined as $\tilde{s}_{q,l}(k) := \mathrm{Re}\{s_{q,l}(k)\}$, for $l = 1, \ldots, L_q$, and $\tilde{s}_{q,l}(k) := \mathrm{Im}\{s_{q,l-L_q}(k)\}$, for $l = L_q + 1, \ldots, 2L_q$. Moreover, splitting the source symbols into real and imaginary parts will also facilitate both the problem formulation and underlying analysis, *regardless of the number of group antennas N_q and symbol constellations*.

[1] Here we only consider $2 \le N_q \le 4$. This is because that the group-wise detection property in the OSIC algorithm will fail for $N_q > 4$ (see Sect. 4). The case $N_q = 1$ can be incorporated but is not included in the deviation; a detailed discussion will be given in Sect. 3.3 instead.

Assume that M ($\geq Q$) antennas are located at the receiver. Let $y_m(k)$ be the received discrete-time signal, sampled at the symbol-rate, from the mth receive antenna and define $\mathbf{y}(k) := [y_1(k), \ldots, y_M(k)]^T \in \mathrm{C}^M$. Collecting $\mathbf{y}(k)$ over K successive symbol periods, we have the following $M \times K$ ST signal model (assuming that the Q antenna groups are symbol synchronized):

$$\mathbf{Y}(k) := \big[\mathbf{y}(k) \cdots \mathbf{y}(k+K-1)\big] = \sum_{q=1}^{Q} \mathbf{H}_q \mathbf{X}_q(k) + \mathbf{V}(k), \tag{3}$$

where $\mathbf{H}_q = \sqrt{P_q}\mathbf{C}_q$, with P_q being the transmit power of the qth antenna group so that $P_1 + P_2 + \cdots + P_Q = P_T$, where P_T is the total transmit power. $\mathbf{C}_q$ is the $M \times N_q$ MIMO matrix channel from the qth antenna group to the receiver, and $\mathbf{V}(k) \in \mathrm{C}^{M\times K}$ is the channel noise. The following assumptions are made in the sequel:

(a1) The symbol streams $s_q(k)$, $q = 1, \ldots, Q$, are i.i.d. with zero-mean and unit-variance, and have the same modulation scheme.
(a2) Equal power allocation is assumed for all antenna groups.
(a3) Each entry of the MIMO matrix channel $\mathbf{C}_q$, $q = 1, \ldots, Q$, is an i.i.d. complex Gaussian random variable with zero-mean and unit-variance, and assumed to be static during the K symbol periods.
(a4) The noise $\mathbf{V}(k)$ is spatially and temporally white, each entry being with zero-mean and variance σ_v^2.
(a5) With $2 \leq N_q \leq 4$, we have $B_q \in \{2, 4\}$ according to O-STBCs.

2.2 Real-valued Vectorized Signal Model

To simplify the detection and analysis process, we propose to use the equivalent linear vector model, based on (3). Specifically, let $\mathbf{s}_q(k) := \big[s_{q,1}(k), \ldots, s_{q,L_q}(k)\big]^T$ be the kth transmitted symbol block of the qth group. Define $\tilde{\mathbf{s}}_q(k) := \Big[\mathrm{Re}\{\mathbf{s}_q^T(k)\}\ \mathrm{Im}\{\mathbf{s}_q^T(k)\}\Big]^T \in \mathrm{R}^{2L_q}$ and $\tilde{\mathbf{y}}(k) := \big[\mathrm{Re}\{\mathbf{y}^T(k)\}\ \mathrm{Im}\{\mathbf{y}^T(k)\}\big]^T \in \mathrm{R}^{2M}$ to be the split real-valued symbol block of the qth antenna group and the received signal vector. Associated with $\mathbf{H}_q$, we form the following augmented matrix:

$$\bar{\mathbf{H}}_q := \mathbf{I}_K \otimes \tilde{\mathbf{H}}_q \in \mathrm{R}^{2KM\times 2KN_q}, \quad q = 1, \ldots, Q, \tag{4}$$

where

$$\tilde{\mathbf{H}}_q := \begin{bmatrix} \mathrm{Re}\{\mathbf{H}_q\} & -\mathrm{Im}\{\mathbf{H}_q\} \\ \mathrm{Im}\{\mathbf{H}_q\} & \mathrm{Re}\{\mathbf{H}_q\} \end{bmatrix} \in \mathrm{R}^{2M\times 2N_q}, \tag{5}$$

and the notation $\otimes$ stands for the Kronecker product. Also define

$$\bar{\mathbf{A}}_q := \begin{bmatrix} \tilde{\mathbf{a}}_{q,1}^{(1)} & \cdots & \tilde{\mathbf{a}}_{q,2L_q}^{(1)} \\ \vdots & \ddots & \vdots \\ \tilde{\mathbf{a}}_{q,1}^{(K)} & \cdots & \tilde{\mathbf{a}}_{q,2L_q}^{(K)} \end{bmatrix} \in \mathrm{R}^{2KN_q\times 2L_q}, \quad q = 1, \ldots, Q, \tag{6}$$

where

$$\tilde{\mathbf{a}}_{q,l}^{(j)} := \left[\mathrm{Re}\left\{\mathbf{a}_{q,l}^{(j)}\right\}^T\ \mathrm{Im}\left\{\mathbf{a}_{q,l}^{(j)}\right\}^T\right]^T \in \mathrm{R}^{2N_q}, \quad j = 1, \ldots, K, \tag{7}$$

with $\mathbf{a}_{q,l}^{(j)}$ denoting the jth column of the matrix $\mathbf{A}_{q,l}$. Then the complex-valued matrix signal model (3) can be rewritten as the following $2KM \times 1$ real-valued vectorized signal model:

$$\mathbf{y}_c(k) := \left[\tilde{\mathbf{y}}(k), \ldots, \tilde{\mathbf{y}}(k+K-1)\right]^T = \mathbf{H}_c \mathbf{s}_c(k) + \mathbf{v}_c(k), \tag{8}$$

where

$$\mathbf{H}_c := \left[\bar{\mathbf{H}}_1 \bar{\mathbf{A}}_1 \cdots \bar{\mathbf{H}}_Q \bar{\mathbf{A}}_Q\right] \in \mathrm{R}^{2KM \times 2L_T} \tag{9}$$

is the equivalent ST channel matrix, $\mathbf{s}_c(k) := \left[\tilde{\mathbf{s}}_1^T(k) \cdots \tilde{\mathbf{s}}_Q^T(k)\right]^T \in \mathrm{R}^{2L_T}$ is the transmitted symbol vector from Q antenna groups, and $\mathbf{v}_c(k) \in \mathrm{R}^{2KM}$ is the corresponding noise component. Then multiplying both sides of (8) from the left by $\mathbf{H}_c^T$ yields the $2L_T \times 1$ "matched-filtered (MF)" signal vector:

$$\mathbf{z}(k) := \mathbf{H}_c^T \mathbf{y}_c(k) = \mathbf{F}\mathbf{s}_c(k) + \mathbf{v}(k), \tag{10}$$

where

$$\mathbf{F} := \mathbf{H}_c^T \mathbf{H}_c \in \mathrm{R}^{2L_T \times 2L_T}, \tag{11}$$

is the matched-filtered channel matrix (MFCM) and $\mathbf{v}(k) := \mathbf{H}_c^T \mathbf{v}_c(k)$. Based on the MF signal $\mathbf{z}(k)$, we can detect the unknown symbols over an observation space of a relatively small dimension. We will hereafter rely on the filtered model (10) for detection.

3 OSIC Detection for Real-valued Constellations

To detect the transmitted symbols, we propose to adopt the algorithm proposed in [25]. For real-valued constellations, by using the distinctive structures of the MFCM $\mathbf{F}$ shown in the following, we will see that the OSIC detector can jointly detect a block of K symbols per iteration associated with a particular antenna group. This is called the "antenna group-wise" OSIC detection property, in the considered G-STBC systems.

3.1 Matched-Filtered Channel Matrix

Before deriving the algorithm, we need to characterize the structures of $\mathbf{F}$. We only show the important results; the detail can be referred to [25]. In the sequel, we denote by $\mathcal{O}(K)$ the set of all $K \times K$ real orthogonal designs with K independent inputs. Also, we denote by $\mathcal{O}(K, L)$ the set of all $K \times K$ real orthogonal designs with L independent inputs.

Lemma 3.1 *Consider the real-valued constellations with $2 \le N_p, N_q \le 4$. According to O-STBCs, we have $K \in \{2, 4\}$. Let $\mathbf{F}_{p,q}$ be the (p,q)th $L_p \times L_q$ block submatrix of $\mathbf{F}$, where $\mathbf{F}$ is defined in (11). Then we have $\mathbf{F}_{q,q} = \alpha_q \mathbf{I}_K$ and $\mathbf{F}_{p,q} \in \mathcal{O}(K)$ whenever $p \ne q$.*

Proof See Appendix A. □

Precisely, Lemma 3.1 specifies that for $p \ne q$:

(p1) For $K = 2$, it turns out $N_1 = N_2 = \cdots = N_Q = 2$. Then $\mathbf{F}_{p,q} \in \mathcal{O}(2)$.
(p2) For $K = 4$ and $N_p = N_q = 2$, each 2×2 block diagonal submatrix of $\mathbf{F}_{p,q} \in \mathrm{R}^{4\times 4}$ belongs to an orthogonal design and each 2×2 block off-diagonal submatrix of $\mathbf{F}_{p,q}$ is a zero matrix. As a result, $\mathbf{F}_{p,q} \in \mathcal{O}(4, 2)$.
(p3) For $K = 4$ and $2 \le N_p, N_q \le 4$ but $N_p \ne N_q \ne 2$, $\mathbf{F}_{p,q} \in \mathcal{O}(4)$.

Table 1 Summary of structures of the MFCM $\mathbf{F}_{p,q}$ for real-valued constellations

Real-valued constellations		
$K = 2$	$N_p = N_q = 2$	$p = q : \mathbf{F}_{qq} = \alpha_q \mathbf{I}_2$
		$p \neq q : \mathbf{F}_{p,q} \in \mathcal{O}(2)$
$K = 4$	$N_p = N_q = 2$	$p = q : \mathbf{F}_{q,q} = \alpha_q \mathbf{I}_4$
		$p \neq q : \mathbf{F}_{p,q} \in R^{4\times 4}$
		$\mathbf{F}_{p,q}^{(1,1)} = \mathbf{F}_{p,q}^{(2,2)} \in \mathcal{O}(2)$;
		$\mathbf{F}_{p,q}^{(1,2)} = \mathbf{F}_{p,q}^{(2,1)} = \mathbf{O}_2$
	$2 \leq N_p, N_q \leq 4$	$p = q : \mathbf{F}_{q,q} = \alpha_q \mathbf{I}_4$
	$N_p \neq N_q \neq 2$	$p = q : \mathbf{F}_{p,q} = \in \mathcal{O}(4)$

Lemma 3.1 is summarized in Table 1, in which we denote by $\mathbf{F}_{p,q}^{(s,t)}$ the (s,t)th block submatrix of $\mathbf{F}_{p,q}$ with a proper dimension. It shows that the block orthogonal structures of $\mathbf{F}$ can substantially be preserved, and the "antenna group-wise" OSIC detection can thus be done.

3.2 Group-wise OSIC Detection

Let us first define $\mathcal{F}_{KL}(L)$ to be the set of all invertible real symmetric $KL \times KL$ matrices, where K and L are two positive integers, so that, for $\mathbf{X} \in \mathcal{F}_{KL}(L)$, with $\mathbf{X}_{k,l}$ being the (k,l)th $K \times K$ submatrix of $\mathbf{X}$, we have $\mathbf{X}_{l,l} = \beta_l \mathbf{I}_K$ and $\mathbf{X}_{k,l} \in \mathcal{O}(K)$ for $k \neq l$. In the following theorem, we will see that $\mathbf{F}^{-1}$, loosely stated, "inherits" the key features of $\mathbf{F}$ established in Lemma 3.1.

Theorem 3.1 *Consider the real-valued constellations with* $2 \leq N_p, N_q \leq 4$ *and hence* $K \in \{2, 4\}$. *Let* $\mathbf{F} \in \mathrm{R}^{L_T \times L_T}$ *be the MFCM as defined in (11). Then each* $K \times K$ *block diagonal submatrix of* $\mathbf{F}^{-1}$ *is a scalar multiple of* $\mathbf{I}_K$ *and each* $K \times K$ *block off-diagonal submatrix of* $\mathbf{F}^{-1}$ *belongs to* $\mathcal{O}(K)$. *This shows that the* KL *diagonal entries of* $\mathbf{F}^{-1}$ *assume* L *distinct levels* β_l, $l = 1, \ldots, L$, *that is*

$$diag\left(\mathbf{F}^{-1}\right) = \{\underbrace{\beta_1, \ldots, \beta_1}_{K \text{ entries}}, \underbrace{\beta_2, \ldots, \beta_2}_{K \text{ entries}}, \ldots, \underbrace{\beta_L, \ldots, \beta_L}_{K \text{ entries}}\}, \tag{12}$$

where $diag(\cdot)$ *denotes the diagonal operation.*

Proof Theorem 3.1 is in fact an immediate result of the following lemma by setting $L = Q$. □

Lemma 3.2 *If* $\mathbf{F} \in \mathcal{F}_{KL}(L)$, *then so is* $\mathbf{F}^{-1}$.

Proof See [26]. □

From (12), based on the zero-forcing (ZF) OSIC detection, we can see that it suffices to search among the L values, one associated with a particular "antenna group" (or a *layer* in the standard V-BLAST detection), for the optimal detection order. Therefore, we can simultaneously detect a block of K symbols at the initial stage.

To compute the optimal indices and corresponding weights (either for ZF criterion or for minimum mean square error (MMSE) criterion as shown in [25]) required in OSIC based

detection, we need to have the explicit knowledge of diagonal entries of $\mathbf{F}_i^{-1}$, where

$$\mathbf{F}_i := \mathbf{H}_{c,i}^T \mathbf{H}_{c,i} \in \mathrm{R}^{K(L-i)\times K(L-i)} \tag{13}$$

is the "deflated" MFCM at the ith iteration, with $\mathbf{H}_{c,i}$ obtained by deleting the associated block(s) of K columns (corresponding to the previously detected signals) from $\mathbf{H}_c$. With such a detect-and-cancel procedure in OSIC followed by an associated linear combining of the resultant signal (10), it can be directly verified that the noise covariance matrix for ZF OSIC is of the form $\mathbf{F}_i^{-1}$ at the ith iteration of OSIC, $i = 1, \ldots, L-1$. Since $\mathbf{F}_i$ is simply obtained by deleting the associated block(s) of K columns and rows from $\mathbf{F}$, we have $\mathbf{F}_i \in \mathcal{F}_{KL}(L-i)$.

From Lemma 3.2, it can be immediately shown that $\mathbf{F}_i^{-1} \in \mathcal{F}_{KL}(L-i)$, and

$$\mathrm{diag}\left(\mathbf{F}_i^{-1}\right) = \{\underbrace{\beta_{i,1}, \ldots, \beta_{i,1}}_{K \text{ entries}}, \underbrace{\beta_{i,2}, \ldots, \beta_{i,2}}_{K \text{ entries}}, \ldots, \underbrace{\beta_{i,L-i}, \ldots, \beta_{i,L-i}}_{K \text{ entries}}\}, \tag{14}$$

where $\beta_{i,l}$ is the lth distinct value distributed on the diagonal of $\mathbf{F}_i^{-1}$. As a consequence, a block of K symbols transmitted from a particular antenna group can be jointly detected at each iteration.

3.3 Incorporation of SM in Proposed G-STBC System

The proposed G-STBC can incorporate the SM encoding scheme as described in [25], in which we treat one antenna as one antenna group for the SM case. The incorporation of SM into the proposed G-STBC system can increase the spectral efficiency by working with an increased number of antenna groups (or data substreams). A price paid for this is that the receiver would then need more antennas in order to have a sufficient number of degrees of freedom for data detection. To realize this mixed-mode structure (G-STBC + SM), we consider the real-valued constellation as described in [25]. In this case, the equivalent matrix $\mathbf{F}$ can be derived as in (10), and has the following properties (see Proposition 3.1 of [25]):

(p1) If $p, q \in S_M$, then each $\mathbf{F}_{p,q} \in \mathrm{R}^{K\times K}$ is a scalar multiple of $\mathbf{I}_K$.
(p2) If $p, q \in S_D$, then $\mathbf{F}_{p,q}$ is as described in Lemma 3.1.
(p3) If $p \in S_D$ and $q \in S_M$, then $\mathbf{F}_{p,q} \in \mathrm{R}^{K\times K}$ belongs $\mathcal{O}(K)$.

It is noteworthy that a scalar multiple of $\mathbf{I}_K$ also belongs to an orthogonal structure. As a result, the implementation issues of group-wise OSIC detection in [25] can also be applied to the G-STBC + SM system. As a demonstration, the possible sets of encoding schemes are listed in Table 4 for $2 \le N \le 8$.

As can be seen from Table 4, the number of possible encoding schemes, or codewords increases significantly as N increases, making the encoding and decoding process a complex task when N is large (codeword selection is done by the receiver). Furthermore, with a large number of antenna groups involved, the number of antennas, and corresponding number of iterations for the OSIC based detection will be large at the receiver. Finally, the SM mode lacks the diversity gain as with the O-STBC mode, and is thus less reliable especially when the user is far from the base station. The above considerations suggest that the proposed G-STBC based scheme is a better choice for the downlink scenario than the mixed-mode alternative.

4 OSIC Detection for Complex-valued Constellations

As presented in Sect. 3.2, when the real symbol constellations are used, the OSIC detection algorithm can be implemented in an "antenna group-wise" manner. However for the complex symbol case, it will be shown below that only a half of a block of $2L_q$ real-valued symbols, (i.e., a block of L_q real-valued symbols) either from the real part or imaginary part of the complex-valued symbols associated with an antenna group may per iteration be jointly detected in OSIC based processing.

4.1 Matched-filtered Channel Matrix

For complex-valued constellations, there are some relevant results essentially different from those in Lemma 3.1. These results will significantly affect the detection framework in OSIC based processing.

Lemma 4.1 *Consider the complex-valued constellations with* $2 \le N_p, N_q \le 4$. *According to O-STBCs, we get* $K \in \{2, 8\}$. *Let* $\mathbf{F}_{p,q}$ *be the* (p, q)*th* $2L_p \times 2L_q$ *block submatrix of* $\mathbf{F}$, *where* $\mathbf{F}$ *is defined in* (*11*). *Then the following results hold.*

(*p1*) *For* $K = 2$, *and* $N_1 = N_2 = \cdots = N_Q = 2$, $\mathbf{F}_{q,q} = \alpha_q \mathbf{I}_4$ *and* $\mathbf{F}_{p,q} \in \mathcal{O}(4)$ *whenever* $p \ne q$.

(*p2*) *For* $K = 8$ *and* $N_p = N_q = 2$, $\mathbf{F}_{q,q} = \alpha_q \mathbf{I}_{16}$ *and* $\mathbf{F}_{p,q} \in \mathrm{R}^{16\times 16}$ *with* $\mathbf{F}_{p,q}^{(s,t)} \in \mathcal{O}(8, 2)$, $s, t = 1, 2$, *whenever* $p \ne q$. *Moreover,* $\mathbf{F}_{p,q}^{(1,1)} = \mathbf{F}_{p,q}^{(2,2)}$ *and* $\mathbf{F}_{p,q}^{(1,2)} = -\mathbf{F}_{p,q}^{(2,1)}$.

(*p3*) *For* $K = 8$ *and* $N_p = 2$, $3 \le N_q \le 4$, $\mathbf{F}_{q,q} = \alpha_q \mathbf{I}_{2L_q}$ *and* $\mathbf{F}_{p,q} \in \mathrm{R}^{16\times 8}$ *with* $\mathbf{F}_{p,q}^{(s,t)} \in \mathcal{O}(4)$, $s = 1, \ldots, 4$, $t = 1, 2$, *whenever* $p \ne q$. *Moreover,* $\mathbf{F}_{p,q}^{(1,1)} = \mathbf{F}_{p,q}^{(2,1)}$, $\mathbf{F}_{p,q}^{(3,1)} = \mathbf{F}_{p,q}^{(4,1)}$, $\mathbf{F}_{p,q}^{(1,2)} = -\mathbf{F}_{p,q}^{(2,2)}$ *and* $\mathbf{F}_{p,q}^{(3,2)} = -\mathbf{F}_{p,q}^{(4,2)}$.

(*p4*) *For* $K = 8$ *and* $3 \le N_p, N_q \le 4$, $\mathbf{F}_{q,q} = \alpha_q \mathbf{I}_8$ *and* $\mathbf{F}_{p,q} \in \mathrm{R}^{8\times 8}$ *with* $\mathbf{F}_{p,q}^{(1,1)} = \mathbf{F}_{p,q}^{(2,2)} \in \mathcal{O}(4)$ *and* $\mathbf{F}_{p,q}^{(1,2)} = \mathbf{F}_{p,q}^{(2,1)} = \mathbf{O}_4$, *whenever* $p \ne q$. *In this case,* $\mathbf{F}_{p,q} \in \mathcal{O}(8, 4)$.

Proof See Appendix B. □

From Lemma 4.1, we have the following results:

1. For $K = 8$ and $N_p = N_q = 2$, $\mathbf{F}_{p,q}^T \mathbf{F}_{p,q} = \mathbf{F}_{p,q} \mathbf{F}_{p,q}^T = c\mathbf{I}_{16}$.
2. For $K = 8$ and $N_p = 2$, $3 \le N_q \le 4$, $\mathbf{F}_{p,q}^T \mathbf{F}_{p,q} = \begin{bmatrix} c_1\mathbf{I}_4 & \mathbf{O}_4 \\ \mathbf{O}_4 & c_2\mathbf{I}_4 \end{bmatrix}$.

The results in Lemma 4.1 are summarized in Table 2. This special structure will no longer allow the "antenna group-wise" OSIC detection framework as described in the real-valued constellations case (see the next section for further explanation).

4.2 Group-wise OSIC Detection

From Lemma 4.1, it can be seen in what follows that $\mathbf{F}_i^{-1}$ no longer inherits the essential structure of $\mathbf{F}_i$. Before investigating the structure of $\mathbf{F}_i^{-1}$, the following definitions are made. Partition the diagonal entries of $\mathbf{F}_i$ into G_i decision groups, with each having the same (nonzero) value, i.e.,

$$\mathrm{diag}\,(\mathbf{F}_i) = \{\underbrace{\alpha_{i,1}, \ldots, \alpha_{i,1}}_{1^{st}\ group:\ \mathcal{G}_{i,1}}, \underbrace{\alpha_{i,2}, \ldots, \alpha_{i,2}}_{2^{nd}\ group:\ \mathcal{G}_{i,2}}, \ldots, \underbrace{\alpha_{i,G_i}, \ldots, \alpha_{i,G_i}}_{G_i^{th}\ group:\ \mathcal{G}_{i,G_i}}\}$$

Table 2 Summary of structures of the MFCM $\mathbf{F}_{p,q}$ for complex-valued constellations

Complex-valued Constellations		
$K = 2$	$N_p = N_q = 2$	$p = q : \mathbf{F}_{qq} = \alpha_q \mathbf{I}_4$
		$p \neq q : \mathbf{F}_{p,q} \in \mathcal{O}(4)$
	$N_p = N_q = 2$	$p = q : \mathbf{F}_{qq} = \alpha_q \mathbf{I}_{16}$
		$p \neq q : \mathbf{F}_{p,q} \in R^{16\times 16}$
		$\mathbf{F}_{p,q}^{(s,t)} \in \mathcal{O}(8,2), 1 \leq s,t \leq 2$
		$\mathbf{F}_{p,q}^{(1,1)} = \mathbf{F}_{p,q}^{(2,2)}; \mathbf{F}_{p,q}^{(1,2)} = -\mathbf{F}_{p,q}^{(2,1)}$
$K = 8$	$N_p = 2$	$p \neq q : \mathbf{F}_{q,q} = \alpha_q \mathbf{I}_{2Lq}$
	$3 \leq N_q \leq 4$	$p \neq q : \mathbf{F}_{p,q} \in R^{16\times 8}$
		$\mathbf{F}_{p,q}^{(s,t)} \in \mathcal{O}(4), 1 \leq s \leq 4, 1 \leq t \leq 2$
		$\mathbf{F}_{p,q}^{(1,1)} = \mathbf{F}_{p,q}^{(2,1)}; \mathbf{F}_{p,q}^{(3,1)} = \mathbf{F}_{p,q}^{(4,1)};$
		$\mathbf{F}_{p,q}^{(1,2)} = -\mathbf{F}_{p,q}^{(2,2)}; \mathbf{F}_{p,q}^{(3,2)} = -\mathbf{F}_{p,q}^{(4,2)}$
	$3 \leq N_p, N_q \leq 4$	$p = q : \mathbf{F}_{q,q} = \alpha_q \mathbf{I}_4$
		$p \neq q : \mathbf{F}_{p,q} \in R^{8\times 8}$
		$\mathbf{F}_{p,q}^{(1,1)} = \mathbf{F}_{p,q}^{(2,2)} \in \mathcal{O}(4); \mathbf{F}_{p,q}^{(1,2)} = \mathbf{F}_{p,q}^{(2,1)} = \mathbf{O}_4$

$$:= \left\{\mathcal{G}_{i,1}, \mathcal{G}_{i,2}, \ldots, \mathcal{G}_{i,G_i}\right\}, \tag{15}$$

Each decision group $\mathcal{G}_{i,g}$, $g = 1, \ldots, G_i$, corresponds to a half of real-valued symbols at the associated antenna group. Hence, each antenna group has two decision groups, each of which has L_q real-valued symbols. Assuming that $\{\alpha_{i,g}\}_{g=1}^{G_i}$ have $D_i(G_i)$ different levels, then $\lceil G_i/2 \rceil \leq D_i(G_i) \leq G_i$, where D_i is a function of G_i. This is because that when the diagonal entries of $\mathbf{F}_i$ have G_i decision groups, there will exist $G_i - \lceil G_i/2 \rceil + 1$ possible outcomes with different levels present on the diagonal of $\mathbf{F}_i$. For concise notation, we drop the dependence of $D_i(G_i)$ on G_i in the following. Besides, let $\mathcal{I}_{i,1}$ and $\mathcal{I}_{i,1/2}$ be respectively the sets of indices of decision group for unit-rate codes and half-rate codes, with $G_{i,1} := |\mathcal{I}_{i,1}|$ and $G_{i,2} := |\mathcal{I}_{i,1/2}|$ denoting the respective cardinalities. Also, let $\mathcal{I}_i := \mathcal{I}_{i,1} \cup \mathcal{I}_{i,1/2}$ be the sets of indices set of both decision groups at the ith iteration, with $G_i := |\mathcal{I}_i|$ denoting the corresponding cardinality. Then we have

$$\mathcal{I}_i = \begin{cases} \mathcal{I}_{i,1} & \text{if } \mathcal{I}_i \cap \mathcal{I}_{i,1/2} = \emptyset \\ \mathcal{I}_{i,1/2} & \text{if } \mathcal{I}_i \cap \mathcal{I}_{i,1} = \emptyset. \end{cases} \tag{16}$$

Next, define $\tilde{\mathcal{F}}_J(G, D)$ to be the set of all invertible real symmetric $J \times J$ matrices, where J, G, D are the positive integers, so that, for $\mathbf{X} \in \tilde{\mathcal{F}}_J(G, D)$, the following hold: (1) each block diagonal submatrix of $\mathbf{X}$ is a (nonzero) scaled identity matrix $\alpha_g \mathbf{I}_{M_g}$, $g = 1, \ldots, G$, with $M_g \in \{2, 4, 8\}$, (2) $\{\alpha_g\}_{g=1}^{G}$ exhibit D different values, with $\lceil G/2 \rceil \leq D \leq G$, (3) for $i, j = 1, \ldots, G, i \neq j$, each 4×4 block submatrix of $M_i \times M_j$ block off-diagonal submatrix of $\mathbf{X}$ belongs to $\mathcal{O}(4)$ or is a zero matrix. Moreover, if $D = G$, then $\tilde{\mathcal{F}}_J(G, D = G)$ can be simplified as $\tilde{\mathcal{F}}_J(G)$.

Theorem 4.1 *Consider the complex-valued constellations. Let* $\mathbf{F}_i \in \mathrm{R}^{J_i \times J_i}$ *be the MFCM and assume that unit-rate and half-rate codes exist at the* i*th detection stage, i.e.,* $\mathcal{I}_i \cap \mathcal{I}_{i,1} \neq \emptyset$ *and* $\mathcal{I}_i \cap \mathcal{I}_{i,1/2} \neq \emptyset$*. At the* i*th iteration, let* $\mathcal{I}_i(g)$*,* $g = 1, \ldots, G_i$ *be the* g*th element of* $\mathcal{I}_i$

and $\mathbf{F}_i \in \mathrm{R}^{J_i \times J_i}$ *the MFCM, where*

$$J_i := \sum_{j \in \mathcal{I}_i} L_{\lceil j/2 \rceil} = \sum_{g=1}^{G_i} L_{\lceil \mathcal{I}_i(g)/2 \rceil}, \tag{17}$$

with $L_q \in \{2, 4, 8\}$ *for all* q. *If* $\mathbf{F}_i \in \tilde{\mathcal{F}}_{J_i}(G_i, D_i)$, *then* $\mathbf{F}_i^{-1} \in \tilde{\mathcal{F}}_{J_i}(G_i)$.

Proof See Appendix C. □

Theorem 4.1 shows that J_i diagonal entries of $\mathbf{F}_i^{-1}$ will assume G_i ($\geq D_i$) distinct levels $\{\beta_{i,g}\}_{g=1}^{G_i}$ (where $\mathbf{F}_i$ only has D_i distinct levels), that is

$$\begin{aligned} \mathrm{diag}\left(\mathbf{F}_i^{-1}\right) &= \{\underbrace{\beta_{i,1}, \ldots, \beta_{i,1}}_{1^{st}\ group:\ \mathcal{G}_{i,1}}, \underbrace{\beta_{i,2}, \ldots, \beta_{i,2}}_{2^{nd}\ group:\ \mathcal{G}_{i,2}}, \ldots, \underbrace{\beta_{i,G_i}, \ldots, \beta_{i,G_i}}_{G_i^{th}\ group:\ \mathcal{G}_{i,G_i}}\} \\ &:= \left\{\mathcal{G}_{i,1}, \mathcal{G}_{i,2}, \ldots, \mathcal{G}_{i,G_i}\right\}. \end{aligned} \tag{18}$$

From (18), it can be seen that it suffices to search among the G_i values, one associated with a particular block of L_q real-valued symbols (i.e., a half of real-valued symbols from the qth antenna group), for the optimal detection order. In contrast, a full set of real-valued symbols that only one block is associated with one antenna group in (14). Based on the same procedures of the group-wise OSIC algorithm (ZF or MMSE criterion) developed for the real-valued constellations, we can thus only simultaneously detect a block of L_q real-valued symbols from a particular antenna group rather than $2L_q$ real-valued symbols at the ith iteration. The same detection scheme holds in the following iterations if the unit-rate and half-rate codes still coexist in those yet-to-be-detected antenna groups. However, when the code rates of all yet-to-be-detected antenna groups are the same, it can be shown according to Theorem 4.1 that the detection property can be simplified to the antenna group-wise detection scheme. That is, it will per iteration jointly detect either a block of L_q or a block of $2L_q$ real-valued symbols depending on the number of symbols remaining in the corresponding yet-to-be-detected antenna group. This thus leads to extra computational complexity. The following is an example for illustrating the possible number of iterations of a G-STBC codeword.

Consider a G-STBC system with eight transmit antenna. A possible G-STBC codeword has the structure in which the $N = 8$ transmit antennas are partitioned into three groups of 2, 2, and 4 antennas with the corresponding code rates being 1, 1, and 1/2, respectively. As a result, the required number of iterations L for optimal ordering performed in OSIC based detection will be $4 \leq L \leq 6$.

5 Implementation Issues of Group-wise OSIC Detection for Complex-valued Constellations

In this section, some implementation issues of the group-wise OSIC detection including the antenna group-wise detection strategy, two-stage detection strategy and a computationally efficient recursive realization are presented to further reduce the receiver complexity. Notice that the implementation of the group-wise OSIC detection for real-valued constellations has been discussed in [25], and here only the complex-valued constellations is considered.

5.1 Antenna Group-wise Detection Strategy

As mentioned in Theorem 4.1, the $2L_{q_i}$ entries distributed on the diagonal of $\mathbf{F}_i^{-1}$ within an antenna group will exhibit two different levels, $\beta_{L_{q_i},1}$ and $\beta_{L_{q_i},2}$. To implement the *antenna group-wise* detection, an intuitive approach is to "directly search" the corresponding decision group index of the diagonal entries of $\mathbf{F}_i^{-1}$ to find the minimum value of the grouped diagonal elements of $\mathbf{F}_i^{-1}$. This is called the direct group-wise method. This is the simplest approach, but will also potentially induce a large detection error. To remedy this, the values $\beta_{q_i,1}$ and $\beta_{q_i,2}$ are averaged within an antenna group as follows:

$$\beta_{i,q} := \frac{\beta_{q_i,1} + \beta_{q_i,2}}{2}, \quad i = 1, \ldots, Q-1, \ q = 1, \ldots, Q-i, \tag{19}$$

and the $\sum_{q=1}^{Q-i} 2L_{q_i}$ diagonal entries of $\mathbf{F}_i^{-1}$ are rewritten as

$$\text{diag}\left(\mathbf{F}_i^{-1}\right) = \{\underbrace{\beta_{i,1}, \ldots, \beta_{i,1}}_{2L_1 \text{ entries}}, \underbrace{\beta_{i,2}, \ldots, \beta_{i,2}}_{2L_2 \text{ entries}}, \ldots, \underbrace{\beta_{i,Q-i}, \ldots, \beta_{i,Q-i}}_{2L_{Q-i} \text{ entries}}\}. \tag{20}$$

Based on $\beta_{i,1}, \ldots, \beta_{i,Q-i}$, we can search the corresponding indices by finding the minimal $\beta_{i,j}$, $j = 1, \ldots, Q-i$ at the ith iteration. This process is called the average group-wise method. Since the detection order thus determined may violate the actual optimal sorting, such a simple processing strategy can reduce the computation at the expense of a possible performance drop. However, as will be seen in the simulation results, the performance drop is not significant.

5.2 Two-stage Detection Strategy

Theoretically, the antenna group that has the higher diversity advantage (i.e., larger N_q or lower rate) is robust against channel impairments and can thus be detected first. Based on this point of view, we propose a "two-stage" detection strategy, in which the low-rate antenna groups (i.e., $N_q = 3$ or $N_q = 4$) are detected first through the group-wise OSIC detection algorithm and then high-rate ones (i.e., $N_q = 2$), to further reduce the detection complexity. Likewise, due to that detection ordering is non-optimal, such a detection strategy may also result in a performance loss, but this performance loss is slight as can be seen in the simulation results. Note that at each processing stage, different code rates may exist, and the proposed "average" or "direct" method can be incorporated.

5.3 Recursive Implementation

To further alleviate the detection complexity, we adopt the recursive algorithm proposed in [25] for implementing the group-wise OSIC detector. However, the method cannot be directly used here and needs some modifications.

In Theorem 4.1, it is shown that the minimum size of an orthogonal matrix in $\mathbf{F}_{p_i,q_i}^{-1}$ is 4×4, where $\mathbf{F}_{p_i,q_i}^{-1} \in \mathrm{R}^{2L_{p_i} \times 2L_{q_i}}$ is the (p,q)th block submatrix of $\mathbf{F}_i^{-1}$. Since the recursion based implementation can only tackle a block orthogonal matrix once at a time, as the matrix dimension of $\mathbf{F}_i$ is large, directly implementing the recursion based processing for the group-wise OSIC detection described above will need more iterations and thus large computational complexity. Fortunately, the two-stage detection strategy can help to reduce the required number of iterations. As a result, in the following we will develop the recursion based implementation incorporating the two-stage detection strategy. Assume that within an

antenna group there are two levels along the diagonal entries of $\mathbf{F}_i^{-1}$ at each iteration. Denote by $\mathbf{F}_i \in \mathrm{R}^{2\left(L_T-\sum_{j=1}^{i} L_{q_j}\right)\times 2\left(L_T-\sum_{j=1}^{i} L_{q_j}\right)}$ the MFCM at the ith iteration, where L_{q_i} is the symbol block length of the qth group to be deleted at the ith iteration. Then $\mathbf{F}_{i-1}$ can be partitioned as

$$\mathbf{F}_{i-1} := \begin{bmatrix} \mathbf{F}_i & \mathbf{B}_{i-1} \\ \mathbf{B}_{i-1}^T & \mathbf{D}_{i-1} \end{bmatrix} \in \mathrm{R}^{2\left(L_T-\sum_{j=1}^{i-1} L_{q_j}\right)\times 2\left(L_T-\sum_{j=1}^{i-1} L_{q_j}\right)}, \tag{21}$$

where $\mathbf{B}_{i-1} \in \mathrm{R}^{2\left(L_T-\sum_{j=1}^{i-1} L_{q_j}\right)\times 2L_{q_{i-1}}}$, and $\mathbf{D}_{i-1} = d_{i-1}\mathbf{I}_{2L_{q_{i-1}}}$, with d_{i-1} being a constant. Denote by $\bar{\mathbf{F}}_{i-1}$ the $2\left(L_T - \sum_{j=1}^{i} L_{q_j}\right) \times 2\left(L_T - \sum_{j=1}^{i} L_{q_j}\right)$ the main submatrix of $\mathbf{F}_{i-1}^{-1}$ and $\mathbf{F}_0^{-1} = \mathbf{F}^{-1}$. From (21) and the inversion lemma for block matrix, $\bar{\mathbf{F}}_{i-1}$ can be expressed as

$$\bar{\mathbf{F}}_{i-1} = \left(\mathbf{F}_i - \mathbf{B}_{i-1}\mathbf{D}_{i-1}^{-1}\mathbf{B}_{i-1}^T\right)^{-1}. \tag{22}$$

In particular, it follows from (22) that

$$\mathbf{F}_i = \bar{\mathbf{F}}_{i-1}^{-1} + \mathbf{B}_{i-1}\mathbf{D}_{i-1}^{-1}\mathbf{B}_{i-1}^T. \tag{23}$$

Using the matrix inversion lemma, we have (after some manipulations)

$$\mathbf{F}_i^{-1} = \bar{\mathbf{F}}_{i-1} - \mathbf{E}_{i-1}\mathbf{C}_{i-1}^{-1}\mathbf{E}_{i-1}^T, \tag{24}$$

where $\mathbf{E}_{i-1} := \bar{\mathbf{F}}_{i-1}\mathbf{B}_{i-1}$, and

$$\mathbf{C}_{i-1} := \mathbf{B}_{i-1}^T\bar{\mathbf{F}}_{i-1}\mathbf{B}_{i-1} + \mathbf{D}_{i-1} = \begin{bmatrix} c_{1,i-1}\mathbf{I}_{L_{q_{i-1}}} & \mathbf{O}_{L_{q_{i-1}}} \\ \mathbf{O}_{L_{q_{i-1}}} & c_{2,i-1}\mathbf{I}_{L_{q_{i-1}}} \end{bmatrix}, \tag{25}$$

for some scalars $c_{j,i-1}$, $j = 1, 2$. In (25), we have used the fact that $\mathbf{B}_{i-1}^T\bar{\mathbf{F}}_{i-1}\mathbf{B}_{i-1}$ has exactly the same structure as that of $\mathbf{C}_{i-1}$ [25]. The result is due to the usage of the orthogonal codes. This provides a simple recursive formula for computing $\mathbf{F}_i^{-1}$ based on $\mathbf{F}_{i-1}$ and $\mathbf{F}_{i-1}^{-1}$ without any direct matrix inversion and this reduces the detection computational load effectively. Note that the good property described in (25) is unique to the two-stage detection. It is also noteworthy that by using the two-stage detection, as all the antenna groups with three or four antennas detected, $\mathbf{C}_{i-1}$ will be a scaled identity matrix i.e., $c_{1,i} = c_{2,i}$.

6 Grouped Space–Time Block Codes

Based on the low-complexity group-wise OSIC detection framework, we will construct the G-STBCs regardless of the number of total transmit antennas N. We then provide a G-STBC codeword selection criterion to suitably choose the G-STBC codewords in accordance with the link performance under the constraints of total transmit power and spectral efficiency.

6.1 G-STBC Codeword Construction and Property

Recall that since L_q symbols are transmitted from the qth antenna group over K symbol periods, or in other words, there are in total L_T data symbols transmitted from N antennas

over K symbol periods, the code rate of the G-STBC is given by

$$R^N := \frac{L_T}{K} = \frac{1}{K}\sum_{q=1}^{Q} \kappa_q B_q$$
$$= \sum_{q=1}^{Q} \frac{B_q}{K_q} = \sum_{q=1}^{Q} R_q^N, \tag{26}$$

where $\kappa_q := K/K_q = L_q/B_q$ is the number of regular O-STBCs, called the *elementary codes*, in the qth antenna group over K symbol periods, and $R_q^N := B_q/K_q$ is the code rate of the qth group code. From (26), we can see that the overall code rate of G-STBC is just the sum of the code rates of Q group codes. As a result, the total "ST area" NK, occupied by the grouped ST codeword will satisfy

$$\sum_{q=1}^{Q} \left(\frac{L_q}{B_q}\right) N_q K_q = \sum_{q=1}^{Q} \kappa_q N_q K_q = NK. \tag{27}$$

For convenient demonstration, the following example is given:

Example Consider $N = 10$, $Q = 4$, antenna group configuration $(N_1, \ldots, N_Q) = (2, 2, 3, 3)$ (one of the possible G-STBC codewords) with complex-valued constellations. The corresponding G-STBC is shown in Fig. 2, in which the total ST area is 80.

Let $\mathcal{S}^N$ be the set of all possible antenna group configurations associated with N transmit antennas and define $J^N := |\mathcal{S}^N|$ to be the respective cardinality, which is the number of all possible sets for constructing an $N \times K$ G-STBC. Here, we define each antenna group configuration of $\mathcal{S}^N$ as a G-STBC codeword. Note that during each symbol block of length K, different antenna group configurations (or G-STBC codewords) can be used for transmission based on the system requirements and/or channel conditions. Moreover, if we define Q_j^N to be the number of antenna groups of the jth possible set for N transmit antennas, then we have

$$\mathcal{S}^N = \left\{\left(N_1, \ldots, N_{Q_j^N}\right)\right\}, \quad j = 1, \ldots, J^N, \tag{28}$$

and $Q_{\min}^N \le Q_j^N \le Q_{\max}^N$, where

$$Q_{\min}^N := \lceil N/4 \rceil \tag{29}$$

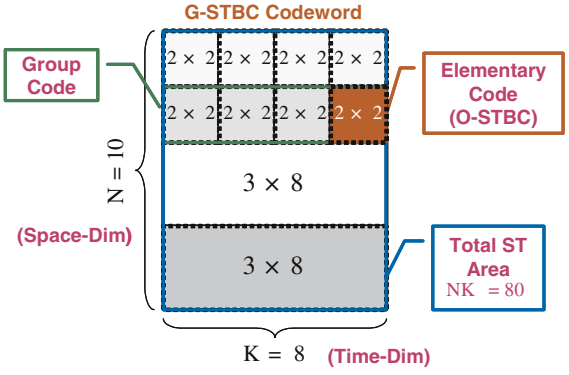

Fig. 2 G-STBC codeword for $N = 10$, $Q = 4$ and $(N_1, \ldots, N_Q) = (2, 2, 3, 3)$ with QPSK modulation

and

$$Q_{\max}^{N} := \lfloor N/2 \rfloor \tag{30}$$

are the respective minimum and maximum numbers of antenna groups over $\mathcal{S}^N$.

For example, when $N = 10$, there are $J^N = 5$ possible antenna group configurations(i.e., 5 possible G-STBC codewords):

$$\mathcal{S}^N = \{\underbrace{(3,3,4)}_{\mathcal{S}_1^N:\ Q_1^N=3},\ \underbrace{(2,4,4)}_{\mathcal{S}_2^N:\ Q_2^N=3},\ \underbrace{(2,2,3,3)}_{\mathcal{S}_3^N:\ Q_3^N=4},\ \underbrace{(2,2,2,4)}_{\mathcal{S}_4^N:\ Q_4^N=4},\ \underbrace{(2,2,2,2,2)}_{\mathcal{S}_5^N:\ Q_5^N=5}\}, \tag{31}$$

and $Q_{\min}^{N} = \lceil N/4 \rceil = 3$, $Q_{\max}^{N} = \lfloor N/2 \rfloor = 5$. The corresponding code structures are shown in Fig. 3. It is noteworthy that the order of the grouped antennas in a G-STBC codeword is not considered for simplicity. As a result, by using the two stage detection strategy, the optimal ordering of the OSIC process may be violated.

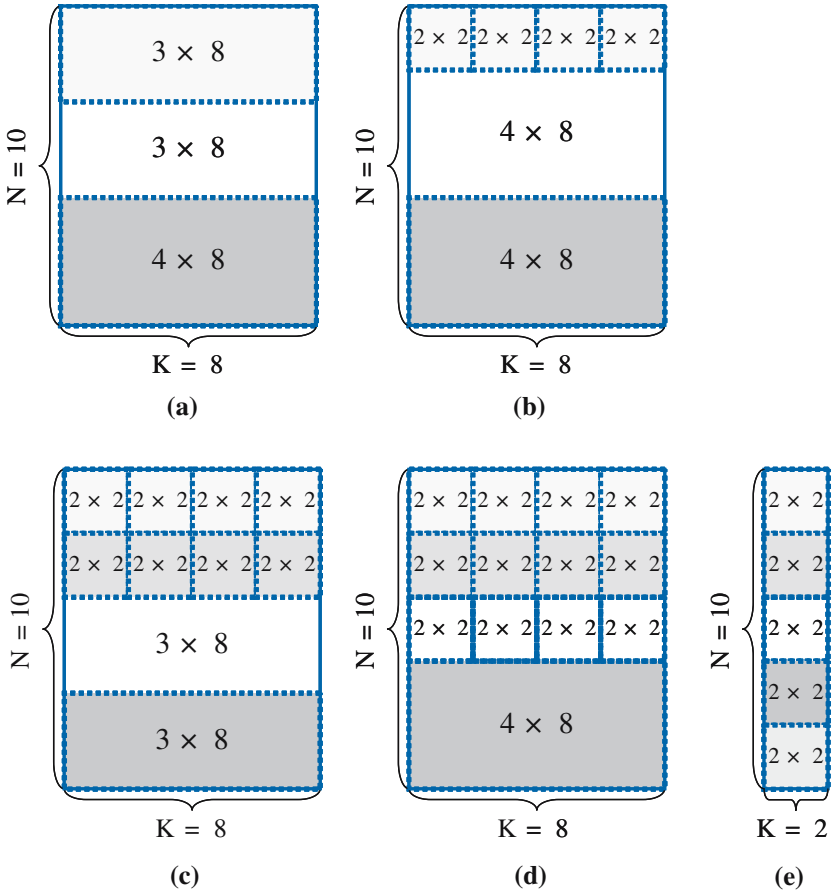

Fig. 3 Five possible $N \times K$ G-STBC codewords with $N = 10$. (**a**) $K = 8$, $Q = 3$, $\mathcal{S}^N = (3, 3, 4)$, $R^N = 1.5$ and $\bar{L}^N = 3$; (**b**) $K = 8$, $Q = 3$, $\mathcal{S}^N = (2, 4, 4)$, $R^N = 2$ and $\bar{L}^N = 6$; (**c**) $K = 8$, $Q = 4$, $\mathcal{S}^N = (2, 2, 3, 3)$, $R^N = 3$ and $\bar{L}^N = 8$; (**d**) $K = 8$, $Q = 4$, $\mathcal{S}^N = (2, 2, 2, 4)$, $R^N = 3.5$ and $\bar{L}^N = 8$; (**e**) $K = 2$, $Q = 5$, $\mathcal{S}^N = (2, 2, 2, 2, 2)$, $R^N = 5$ and $\bar{L}^N = 5$

With above examples, some observations regarding the G-STBC codeword properties are given as follows.

(a) *Code rate:* For a fixed N, different G-STBC codewords may lead to different code rates even under the same number of antenna groups.
(b) *Diversity advantages:* Different transmit diversity gains are provided by different G-STBC codewords leading to different BER performances.
(c) *Computational complexity:* Different G-STBC codewords will also lead to different computational loads at the receiver.

As a result, for a fixed N, the characteristics of G-STBC codeword including code rate, BER performance and receiver computational complexity will be significantly affected by the antenna group configuration. Based on above discussions, we can conclude that an optimal selection of G-STBC codeword, namely G-STBC codeword selection, that can achieve the best system performance should jointly consider code rate, BER performance and receiver computational complexity. Table 3 shows all possible G-STBC codewords, the corresponding code rate R^N and maximum required number of iterations $\bar{L}^N$ for group-wise OSIC with the number of total transmit antennas ranging from $N = 2$ to $N = 16$.

6.2 G-STBC Codeword Selection Criterion

As mentioned above, G-STBC codeword selection is a very critical issue to the overall system performance. The code rate, modulation type, diversity advantage and detection complexity should be jointly considered at the receiver to efficiently determine an optimal G-STBC codeword (antenna configuration). We refer to a combination of specific G-STBC codeword and modulation as a *mode*, which is similar to the definition in [27]. Denote by $\mathcal{M}_j^N$ the jth mode of all possible mode candidates for N transmit antennas, and $\eta\left(\mathcal{M}_j^N\right)$ the corresponding spectral efficiency. Here the same modulation, e.g., $\bar{M}$-ary PSK or $\bar{M}$-ary QAM modulation, is considered for all antenna groups, that is $R_{b,1} = \cdots = R_{b,Q} := R_b$, where $R_{b,q}$ is the bit rate of the qth group. As a result, the spectral efficiency of the jth mode can be represented as

$$\begin{aligned}\eta\left(\mathcal{M}_j^N\right) &= \sum_{q=1}^{Q} R_q^N(j) R_{b,q}(j) \\ &= R_b(j) \sum_{q=1}^{Q} R_q^N(j) = R_b(j) R^N(j) \qquad \text{(bits/sec/Hz)}, \end{aligned} \tag{32}$$

where $R_{b,q}(j)$ is the qth group's bit rate of the jth mode and $R^N(j) = \sum_{q=1}^{Q} R_q^N(j)$ is the total code rate of the jth mode. This shows that the spectral efficiency $\eta\left(\mathcal{M}_j^N\right)$ varies with the code rate R^N and transmission bit rate R_b, and these two parameters can be appropriately adjusted to achieve the desired spectral efficiency. Equivalently, specifying the codeword and modulation type will define the overall spectral efficiency.

Since the antenna group-wise detection strategy can reduce the detection complexity significantly with an acceptable performance drop, in the following, we will design the G-STBC codeword selection criterion under this detection strategy. Then the optimal mode selection criterion under the given signal-to-noise ratio (SNR) constraint and spectral efficiency $\eta\left(\mathcal{M}_j^N\right)$ can be found by searching the index of candidate modes at which the corresponding

Table 3 Possible sets of G-STBC codeword and corresponding code rate and maximum required number of iterations for group-wise OSIC detection

N	J^N	Possible sets of antenna configuration, $\mathcal{S}^N$	Coding rates, R^{N*}	Max number of iterations, $\bar{L}^{N*}$
2	1	(2)	1	1
3	1	(3)	0.5	1
4	2	(4), (2,2)	0.5, 2	1, 2
5	1	(2,3)	1.5	4
6	3	(3,3), (2,4), (2,2,2)	1, 1.5, 3	2, 4, 3
7	2	(3,4), (2,2,3)	1, 2.5	2, 6
8	4	(4,4), (2,3,3), (2,2,4), (2,2,2,2)	1, 2, 2.5, 4	2, 6, 6, 4
9	3	(3,3,3), (2,3,4), (2,2,2,3)	1.5, 2, 3.5	6, 3, 8
10	5	(3,3,4), (2,4,4), (2,2,3,3), (2,2,2,4), (2,2,2,2,2)	1.5, 2, 3, 3.5, 5	3, 6, 8, 8, 5
11	4	(3,4,4), (2,3,3,3), (2,2,3,4), (2,2,2,2,4)	1.5, 2.5, 3, 4.5	3, 8, 8, 10
12	7	(4,4,4), (3,3,3,3), (2,3,3,4), (2,2,4,4), (2,2,2,3,3), (2,2,2,2,4), (2,2,2,2,2,2)	1.5, 2, 2.5, 3, 4, 4.5, 6	3,4, 8, 8, 10, 10,6
13	5	(3,3,3,4), (2,3,4,4), (2,2,3,3,3), (2,2,2,3,4), (2,2,2,2,2,3)	2, 2.5, 3.5, 4, 5.5	4, 8, 10, 10, 12
14	8	(3,3,4,4), (2,4,4,4), (2,3,3,3,3), (2,2,3,3,4), (2,2,2,4,4), (2,2,2,2,3,3), (2,2,2,2,2,4), (2,2,2,2,2,2,2)	2, 2.5, 3, 3.5, 4, 5, 5.5, 7	4, 8, 10, 10, 10, 12, 12, 7
15	7	(3,4,4,4), (3,3,3,3,3), (2,3,3,3,4), (2,2,3,4,4), (2,2,2,3,3,3), (2,2,2,2,3,4), (2,2,2,2,2,2,3)	2, 2.5, 3, 3.5, 4.5, 5, 6.5	4, 5, 10, 10, 12, 12, 14
16	10	(4,4,4,4), (3,3,3,3,4), (2,3,3,4,4), (2,2,4,4,4), (2,2,3,3,3,3), (2,2,2,3,3,4), (2,2,2,2,4,4), (2,2,2,2,2,3,3), (2,2,2,2,2,2,4), (2,2,2,2,2,2,2,2)	2, 2.5, 3, 3.5, 4, 4.5, 5, 6, 6.5, 8	4, 10, 10, 10, 12, 12, 12, 14, 14, 8

* For complex-valued symbol constellations

BER performance is minimal:

$$j = \arg \min_{\forall\, j} P_e \left(\mathcal{M}_j^N \mid \left\{ \text{SNR}, \eta \left(\mathcal{M}_j^N \right) \right\} \right). \tag{33}$$

Since spectral efficiency is a function of the code rate R^N and transmission bit rate R_b, for a fixed spectral efficiency, specifying R_b (i.e., modulation type) will determine R^N or the G-STBC codeword. Hence, the jth G-STBC codeword is selected if

$$j = \arg \min_{\forall\, j} P_e \left(\mathcal{S}_j^N \mid \{P_T, R_b(j)\} \right). \tag{34}$$

This shows that the optimal G-STBC codeword is chosen from j-th G-STBC codeword set $\mathcal{S}_j^N$ to minimize BER, under the constraints of total transmit power P_T and transmission

bit rate R_b. As a result, only a few bits, indicating the G-STBC codeword and associated modulation type, are required to be fed back from the receiver to transmitter for choosing the optimal G-STBC codeword.

The average BER P_e can be calculated as follows:

$$P_e(j) = \frac{1}{\eta\left(\mathcal{M}_j^N\right)} \sum_{q=1}^{Q} \left(R_q^N(j) R_{b,q}(j)\right) P_{e,q}(j) = \frac{1}{R^N(j)} \sum_{q=1}^{Q} R_q^N(j) P_{e,q}(j), \quad (35)$$

where $P_{e,q}(j)$ is the BER of the qth antenna group. By ignoring the error propagation effect in OSIC detection, $P_{e,q}(j)$ can be approximated as a function of the post-detected signal-to-interference-plus-noise ratio (SINR) γ_q depending on the adopted detection criterion and transmission bit rate of the qth group $R_{b,q}$:

$$P_{e,q}(j) \approx g_{\gamma,R_b}\left(\gamma_q(j), R_{b,q}(j)\right), \quad (36)$$

with

$$\gamma_q(j) = \begin{cases} 1/\sigma_{v,q}^2(j) & \text{ZF criterion} \\ \left(1-\varepsilon_q(j)\right)/\varepsilon_q(j) & \text{MMSE criterion} \end{cases} \quad (37)$$

where $\sigma_{v,q}^2(j) := \frac{\sigma_v^2}{2} \mathbf{e}_{q_i}^T \left[\mathbf{H}_{c,i}^T(j)\mathbf{H}_{c,i}(j)\right]^{-1} \mathbf{e}_{q_i}$ and $\varepsilon_q(j) := \mathbf{e}_{q_i}^T \left[\frac{2}{\sigma_v^2}\mathbf{H}_{c,i}^T(j)\mathbf{H}_{c,i}(j) + \mathbf{I}\right]^{-1}$ $\mathbf{e}_{q_i}$ are the output noise power and symbol MSE of the qth antenna group at the ith iteration of OSIC detection, where $\mathbf{H}_{c,i}$ is defined in (13) and $\mathbf{e}_l$ the lth unit standard vector in R^{L_T}. From (36) and (37), it can be seen that the BER performance greatly depends on the detection metric. When the uncoded $\bar{M}$-ary QAM modulation is used for all transmitted symbols, according to [28], the BER of the qth antenna group can be tightly approximated as

$$\begin{aligned} g_{\gamma,R_b}\left(\gamma_q(j), R_{b,q}(j)\right) &\approx \frac{2}{R_{b,q}(j)}\left(1-\frac{1}{\sqrt{2^{R_{b,q}(j)}}}\right)\mathrm{erfc}\left(\sqrt{\frac{1.5\gamma_q(j)}{2^{R_{b,q}(j)}-1}}\right) \\ &= \begin{cases} \frac{2}{R_{b,q}(j)}\left(1-\frac{1}{\sqrt{2^{R_{b,q}(j)}}}\right)\mathrm{erfc}\left(\sqrt{\frac{1.5}{\left(2^{R_{b,q}(j)}-1\right)\sigma_{v,q}^2(j)}}\right) & \text{ZF} \\ \frac{2}{R_{b,q}(j)}\left(1-\frac{1}{\sqrt{2^{R_{b,q}(j)}}}\right)\mathrm{erfc}\left(\sqrt{\frac{1.5\left(1-\varepsilon_q(j)\right)}{\left(2^{R_{b,q}(j)}-1\right)\varepsilon_q(j)}}\right) & \text{MMSE} \end{cases} \end{aligned} \quad (38)$$

where $2^{R_{b,q}(j)} = \bar{M}$ and $\mathrm{erfc}(\cdot)$ is the complementary error function.

Based on the results of mathematical analysis, the optimal G-STBC codeword selection algorithm in the minimum BER sense under the constraints of total transmit power and required SE is summarized as follows:

- Choose the number of total transmit antennas N, and give the total transmit power P_T and required data rate R_b.
- For a fixed N, choose the codeword candidates according to Table 4 under the constraints of total transmit power P_T and required data rate R_b.
- According to the channel characteristics, select the optimal G-STBC codeword based on the minimum BER performance through the analysis results in (35–38).

Table 4 Possible sets of codewords for mixed-mode system (G-STBC + SM)

N	J^N	Possible sets of G-STBC codewords, $\mathcal{S}^N$	Coding rates, R^{N*}	Max # iters, $\bar{L}^{N*}$
2	2	(1,1), (2)	2, 1	2, 1
3	3	(1,1,1), (2,1), (3)	3, 2, 0.5	3, 2, 1
4	5	(1,1,1,1), (1,1,2), (2,2), (1,3), (4)	4, 3, 2, 1.5, 0.5	4, 3, 2, 4, 1
5	6	(1,1,1,1,1), (1,1,1,2), (1,2,2), (1,1,3), (1,4), (2,3)	5, 4, 3, 2.5, 1.5, 1.5	5, 4, 3, 6, 4, 4
6	9	(1,1,1,1,1,1), (1,1,1,1,2), (1,1,2,2), (1,1,1,3), (2,2,2), (1,1,4), (1,2,3), (2,4), (3,3)	6, 5, 4, 3.5, 3, 2.5, 2.5, 1.5, 1	6, 5, 4, 8, 3, 6, 6, 4, 2
7	11	(1,1,1,1,1,1,1), (1,1,1,1,1,2), (1,1,1,2,2), (1,1,1,1,3), (1,2,2,2), (1,1,1,4), (1,1,2,3), (1,2,4), (2,2,3), (1,3,3), (3,4)	7, 6, 5, 4.5, 4, 3.5, 3.5, 2.5, 2.5, 2, 1	7, 6, 5, 10, 8, 8, 8, 6, 6, 6, 2
8	15	(1,1,1,1,1,1,1,1), (1,1,1,1,1,1,2), (1,1,1,1,2,2), (1,1,1,1,1,3), (1,1,2,2,2), (1,1,1,1,4), (1,1,1,2,3), (2,2,2,2), (1,1,2,4), (1,2,2,3), (1,1,3,3), (2,2,4), (1,3,4), (2,3,3), (4,4)	8, 7, 6, 5.5, 5, 4.5, 4.5, 4, 3.5, 3.5, 3, 2.5, 2, 2, 1	8, 7, 6, 12, 5, 10, 10, 4, 8, 8, 8, 6, 6, 6, 2

* For complex-valued symbol constellations

7 Computer Simulations

Computer simulations are conducted to evaluate the performance of the proposed closed-loop G-STBC in a packet data system. The fading channels between the transmitter and receiver are assumed to be quasi-static, remaining constant over each packet of 100 symbol blocks and independently varying between packets. Perfect channel information is assumed to be available at the receiver but not at the transmitter. In all simulations, unless otherwise mentioned, QPSK modulation is used. Finally, all antenna groups are assumed to be of equal power and SNR $:= P_T/\sigma_v^2$ is the average SNR regardless of the number of total transmit antennas and number of antenna groups. Besides, the maximum number of iterations in OSIC detection is defined as $\bar{L}^N$.

The first set of simulations evaluates the performance of the proposed OSIC detection method (as described in Sect. 4) and compares it with the Naguib's method [19] and Stamoulis's method [20]. In this simulation, $Q = 3$, $M = 3$, and $N = 6$ with $\mathcal{S}^N = (2, 2, 2)$ ($\bar{L}^N = 3$) are assumed. Figure 4 plots the BER performances of the three detection methods as a function of SNR. As shown in this figures, the Stamoulis's method is less favorable since it is a pure decoupling based algorithm and does not enjoy the increased receive diversity gain, even with the power ordering strategy incorporated [25]. Similar result is also observed for the Naguib's one-step method. However, the Naguib's two-step method provides considerable performance improvement at low SNR, but exhibits performance degradation at medium-to-high SNR. This is because that the detection accuracy in the second stage hinges entirely on the reliability of all the initial signal estimates in the Naguib's two-step method.

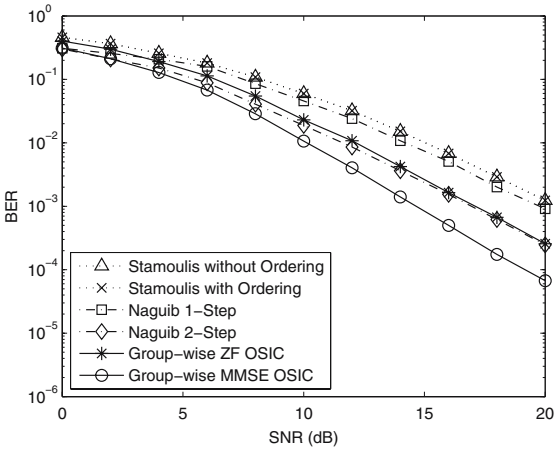

Fig. 4 BER performances of different detection methods as a function of SNR with $M = 3$ and $Q = 3$, $N = 6$ and $\mathcal{S}^N = (2, 2, 2)$

Accordingly, each group's symbol stream, detected via the PIC based mechanism, would be subject to an essentially equal risk of error propagation resulting from incorrect decisions in the initial stage. On the other hand, OSIC based methods enjoy an increase in receive diversity gain, which helps limit the effect of possible decision error propagation [25]. The results also show that, in most SNR regions, the proposed method can successfully suppress the interference and achieve a large diversity gain through the SIC scheme. In the rest of simulations, only the ZF based OSIC detection is considered for simplicity.

In the second set of simulations, the performance of several detection strategies, i.e., the proposed antenna group-wise detection strategies (as described in Sect. 5.1, including the average group-wise method and direct group-wise method) and the two-stage detection strategy (as described in Sect. 5.2), respectively, are evaluated for $N = 8$, $M = 3$, $Q = 3$ and $\mathcal{S}^N = (2, 2, 4)$. Also, the original group-wise OSIC detection method with optimal ordering as described in Section 4.2 is included for comparison. Note that the number of iterations is $L = 3$ for antenna group-wise detection and two-stage detection due to $Q = 3$. However, the required number of iterations for the group-wise OSIC with optimal ordering is $4 \leq L \leq 6$ due to the possible existence of different code rates at each iteration (see Sect. 4.2). The BER performance results are plotted in Fig. 5. It is observed that the two-stage and antenna group-wise detection strategies exhibit a slight performance degradation compared with the proposed method with the maximum number of iterations (about 1.5 dB for the two-stage scheme and $0.5 \sim 1$ dB for the antenna group-wise scheme at 10^{-5} BER performance) due to the insufficient iterations and non-optimal detection ordering in OSIC based detection (as described in Sect. 5.1 and 5.2). Also as expected, the performance of the average method is superior to that of the direct group-wise method. It is noteworthy that the average BER performance of group-wise ZF OSIC in Fig. 5 is significantly better than that in Fig. 4. This is due to that the average BER performance of OSIC detection is dominated by the BER of the first substream. In this simulation, the first substream with $\mathcal{S}^N = (2, 2, 4)$ enjoys twice the diversity gain of the first substream in Fig. 4, leading to a lower average BER. For simplicity, in the following simulations, only the two-stage method incorporating the average antenna group-wise scheme is considered for signal detection.

The third set of simulations investigates the performance of the proposed G-STBCs (as described in Sect. 6.1) compared to various transmission schemes: conventional SM scheme with ZF OSIC detection, O-STBC scheme with ML decoding, A00B scheme, and ABBA

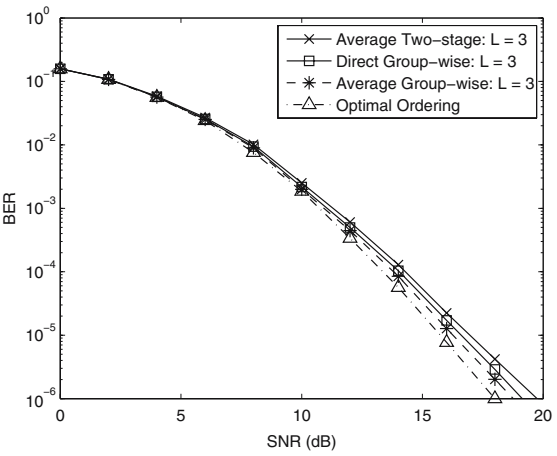

Fig. 5 BER performance of different detection strategies of proposed OSIC detector as a function of SNR with $N = 8$, $M = 3$, $Q = 3$ and $\mathcal{S}^N = (2, 2, 4)$

scheme for $N = M = 4$. The O-STBC scheme with rate $1/2$ which maintains the orthogonal property is described in [13]. The A00B scheme is a space-time code in which two symbols are transmitted from antennas 1, 2 at the first block duration and then two different symbols are transmitted from antenna 3,4 at the second block duration. The ABBA scheme [29] divides four antennas into two groups, with each group encoded by O-STBC. As a result, the ABBA and A00B schemes can be regarded as variations of the proposed G-STBC for the (2,2) configuration. In this simulation, the total spectral efficiency is constrained to $\eta = 4$ (bits/sec/Hz). As a result, BPSK, 256-QAM, 16-QAM, 16QAM modulations are adopted for the conventional SM, O-STBC, A00B, and ABBA, respectively. On the other hand, for the proposed G-STBC, $\mathcal{S}^N = (2, 2)$ ($Q = 2$) with QPSK is considered. The BER performances of those transmission techniques as a function of SNR are plotted in Fig. 6. It can be seen that the conventional STBC technique has a performance limit due to the usage of high order QAM modulation. The conventional SM technique exhibits poor BER performance especially in the medium-to-high SNR regions due to fewer degrees-of-freedom for interference suppression and poorer diversity advantages (no TD gain). The proposed rate-two G-STBC scheme achieves the same transmit diversity order of two as that of A00B scheme, but exhibits better performance at all SNR cases. In addition, it is seen that the ABBA scheme outperforms the half-rate O-STBC for all SNR regions; this is achieved at the cost of a higher decoding complexity. However, the ABBA scheme exhibits some performance degradation compared to the proposed (2,2) G-STBC (rate-two) at the medium SNR region. This shows that the proposed G-STBC provides better trade-off between diversity and code rate compared to the fixed rate one non-orthogonal codes. The results also show the flexibility of the proposed technique in selecting the G-STBC codeword and modulation type to achieve better performance.

Finally, the performance of the proposed G-STBC codewords for a fixed N is examined. In this simulation, the BER obtained by the mathematical analysis in (35–38) is also included. In the first experiment, $N = 6$ and $M = 3$ are considered. As a result, according to Table 4, there are three possible G-STBC codewords (or antenna configuration sets), which are: $\mathcal{S}_1^N = (3, 3)$ ($Q = 2$), $\mathcal{S}_2^N = (2, 4)$ ($Q = 2$), and $\mathcal{S}_3^N = (2, 2, 2)$ ($Q = 3$) with the corresponding code rates being $R^N = 1$, 1.5 and 3, respectively. Assume that the total spectral efficiency is constrained to be $\eta = 6$ (bits/sec/Hz). To meet this spectral efficiency constraint, 64-QAM, 16-QAM, and QPSK modulations are respectively adopted for the above

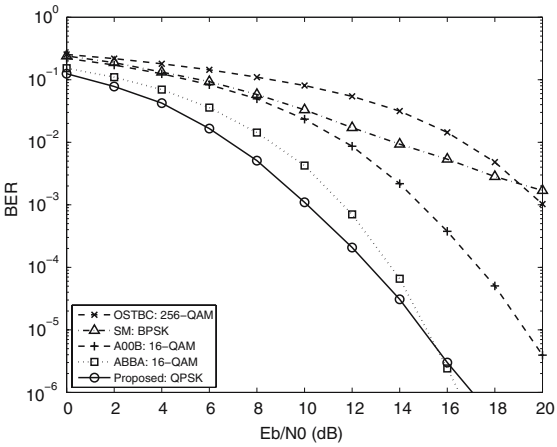

Fig. 6 BER performance of different transmission techniques as a function of SNR with $N = 4$ and $M = 4$

three G-STBC codewords. As observed in Fig. 7a, the curves of mathematical analysis for all codeword cases are nearly the same as those of simulation results. Figure 7a also shows that, $\mathcal{S}_2^N = (2, 4)$ achieves the best BER performance at medial-to-high SNRs. However, for lower SNR, $\mathcal{S}^N = (2, 2, 2)$ may be the best candidate. In the second experiment, $N = 8$ and $M = 4$ are assumed and the results are plotted in Fig. 7b. $\eta = 4$ (bits/sec/Hz) is assumed in this scenario. From Table 4 and under the total spectral efficiency constraint, the following three G-STBC codewords are adopted for comparison: $\mathcal{S}_1^N = (4, 4)$ ($Q = 2$), $\mathcal{S}_2^N = (2, 3, 3)$ ($Q = 3$), and $\mathcal{S}_3^N = (2, 2, 2, 2)$ ($Q = 4$), with the respective modulation types being 16-QAM, QPSK, and BPSK, respectively. Again, the mathematical analysis is consistent with the simulation result. For a large L, however, a slight difference between the analysis and simulation results occurs. This may be due to the approximation in (38) and the assumption of ignoring the error propagation effects in the OSIC detection algorithm for the analytic derivation. Based on the observations, the best G-STBC codeword can thus be selected in accordance with the analytic BER performance as follows: $\mathcal{S}_3^N = (2, 2, 2, 2)$ for low SNRs ($\leq$2 dB), $\mathcal{S}_1^N = (2, 3, 3)$ for moderate SNRs (2 $\sim$ 14 dB) and $\mathcal{S}_2^N = (4, 4)$ for high SNRs ($\geq$14 dB). Based on the analytical BER, the best G-STBC codeword can be chosen for different SNR values.

8 Conclusion

In this paper, an efficient closed-loop MIMO transceiver with limited feedback overhead is proposed for the downlink over Rayleigh flat-fading channels. In the transmitter, a grouped STBC with an arbitrary number of transmit antennas is presented for achieving a high link quality and high spectral efficiency. In particular, the transmit antennas are partitioned into several groups with each being individually encoded by the orthogonal STBC. The proposed encoding strategy reduces the number of receive antennas required at the user terminal, meeting the practical consideration in implementation cost and physical size. At the receiver, based on the distinctive structures of the matched-filtered channel matrix, it is shown that an appealing antenna group-wise OSIC detection property, by which a block of symbols associated with an antenna group can be jointly detected per iteration, is allowed for real-valued symbols. This detection strategy, however, cannot be realized for complex-valued

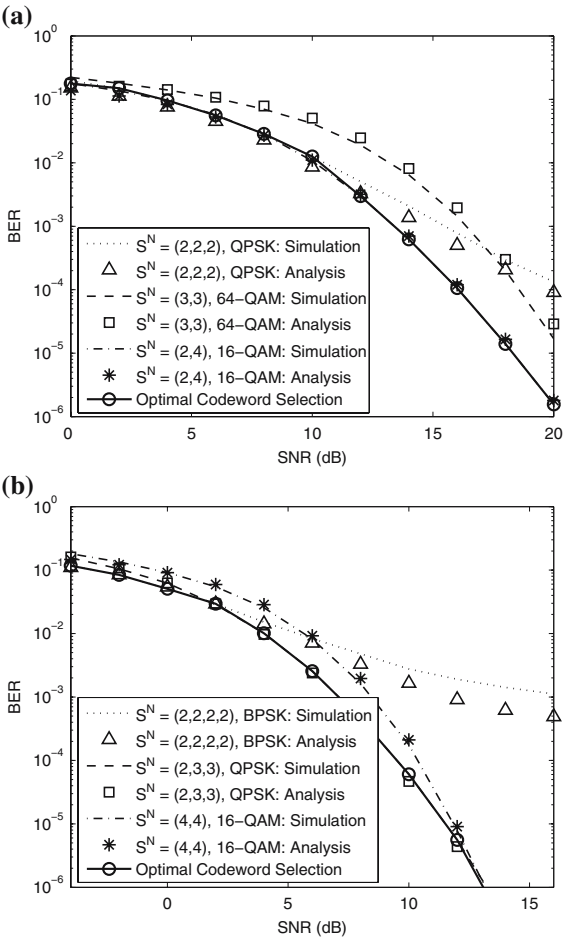

Fig. 7 BER performance of different G-STBC codewords as a function of SNR. (**a**) $N = 6$ and $M = 3$; (**b**) $N = 8$ and $M = 4$

symbols. To tackle this problem, an average antenna group-wise detection approach and a two-stage scheme are then proposed to reduce the detection complexity with the expense of a small performance drop. Moreover, to further alleviate the detection computational load, a recursion based implementation of the developed antenna group-wise OSIC detector is presented by using the algebraic properties of orthogonal codes. Next, based on the group-wise OSIC detection property, allowable G-STBC codewords of grouped STBCs regardless of the number of transmit antennas can be determined. The G-STBC codeword properties are also discussed and a simple selection criterion for choosing the optimal G-STBC codeword is designed based on the minimum BER criterion under the constraints of total transmit power and data throughput. Finally, simulation results show that the proposed G-STBC coding technique can flexibly and judiciously select the G-STBC codewords and associated modulation types to achieve a good trade-off between the spatial multiplexing and transmit diversity techniques.

Acknowledgements This work is sponsored jointly by National Science Council of Taiwan under grant NSC 95-2752-E-002-009, by the Ministry of Education of Taiwan under the MoE ATU Program, and by Media Tek research center at National Chiao Tung University, Taiwan.

Appendix

A Proof of Lemma 3.1

Part (p1) of Lemma 3.1 has been shown in [24]. It only remains to prove Parts (p2–p3).

Proof of (p2) From (9), it can be seen that the effective signal component (prior to matched filtering) of the qth antenna group is $\bar{\mathbf{H}}_q\bar{\mathbf{A}}_q$. Accordingly, the MFCM coupling signature between the pth and qth antenna groups is $\bar{\mathbf{A}}_p^T\bar{\mathbf{H}}_p^T\bar{\mathbf{H}}_q\bar{\mathbf{A}}_q$, whose (i,j)th entry, $i,j=1,\ldots,L_q$, is directly computed as

$$\begin{aligned} f_{p,q}^{(i,j)} &= \sum_{k=1}^{K}\left(\tilde{\mathbf{a}}_{p,i}^{(k)}\right)^T\tilde{\mathbf{H}}_p^T\tilde{\mathbf{H}}_q\tilde{\mathbf{a}}_{q,j}^{(k)} = \sum_{k=1}^{K}\mathrm{Re}\left\{\left(\mathbf{a}_{p,i}^{(k)}\right)^H\mathbf{H}_p^H\mathbf{H}_q\mathbf{a}_{q,j}^{(k)}\right\} \\ &= \sum_{k=1}^{K}\mathrm{Re}\left\{\sum_{m=1}^{M}\mathbf{h}_{p,m}^H\mathbf{a}_{p,i}^{(k)}\left(\mathbf{a}_{q,j}^{(k)}\right)^H\mathbf{h}_{q,m}\right\} \\ &= \mathrm{Re}\left\{\sum_{m=1}^{M}\mathbf{h}_{p,m}^H\left[\sum_{k=1}^{K}\mathbf{a}_{p,i}^{(k)}\left(\mathbf{a}_{q,j}^{(k)}\right)^H\right]\mathbf{h}_{q,m}\right\} \\ &= \mathrm{Re}\left\{\sum_{m=1}^{M}\mathbf{h}_{p,m}^H\mathbf{A}_{p,i}\mathbf{A}_{q,j}^H\mathbf{h}_{q,m}\right\}, \end{aligned} \tag{39}$$

where $\mathbf{h}_{q,m}^T$ is the mth row of $\mathbf{H}_q$. Equation 39 gives an important observation that the (i,j)th element of $\mathbf{F}_{p,q}$ fully describing the structure of $\mathbf{F}_{p,q}$ is completely characterized by $\mathbf{A}_{p,i}$ and $\mathbf{A}_{q,j}$, or simply $\mathbf{A}_{p,i}\mathbf{A}_{q,j}^H$. As a result, to see the particular structure of $\mathbf{F}_{p,q}$, we need to first compute $\mathbf{A}_{p,i}\mathbf{A}_{q,j}^H$. For $N_p=N_q=2$, and according to [13], we have

$$\begin{aligned} &\mathbf{A}_{p,1}=\mathbf{A}_{q,1}=\begin{bmatrix}1&0&0&0\\0&1&0&0\end{bmatrix}, \quad \mathbf{A}_{p,2}=\mathbf{A}_{q,2}=\begin{bmatrix}0&-1&0&0\\1&0&0&0\end{bmatrix}, \\ &\mathbf{A}_{p,3}=\mathbf{A}_{q,3}=\begin{bmatrix}0&0&1&0\\0&0&0&1\end{bmatrix}, \quad \mathbf{A}_{p,4}=\mathbf{A}_{q,4}=\begin{bmatrix}0&0&0&-1\\0&0&1&0\end{bmatrix}. \end{aligned} \tag{40}$$

From (39) and (40) and using the property of O-STBC, it can be easily checked that the (i,j)th entry of $\mathbf{F}_{p,q}$ will be zero except for the following entries:

$$\begin{cases} f_{p,q}^{(1,1)}=f_{p,q}^{(2,2)}, & f_{p,q}^{(1,2)}=-f_{p,q}^{(2,1)}, \\ f_{p,q}^{(3,3)}=f_{p,q}^{(4,4)}, & f_{p,q}^{(3,4)}=-f_{p,q}^{(4,3)}, \\ f_{p,q}^{(1,1)}=f_{p,q}^{(3,3)}, & f_{p,q}^{(2,2)}=f_{p,q}^{(4,4)}. \end{cases} \tag{41}$$

Likewise, for $i,j=1,\ldots,4$, we can also obtain $f_{q,q}^{(i,i)}=\alpha_q$ and $f_{q,q}^{(i,j)}=0$ whenever $i\neq j$. Based on the above results, Part (p2) is asserted. □

Proof of (p3) For $N_p=N_q=3$ and $N_p=N_q=4$, the assertions have been proved in [24]. The cases remaining to be proved are those ones for (a) $N_p=2$, $3\leq N_q\leq 4$ and (b) $N_p=3$, $N_q=4$. Now, we first consider case (a). In particular, for $N_q=4$, we have

$$\mathbf{A}_{q,1}=\mathbf{I}_4, \mathbf{A}_{q,2}=\begin{bmatrix}0&-1&0&0\\1&0&0&0\\0&0&0&1\\0&0&-1&0\end{bmatrix}, \quad \mathbf{A}_{q,3}=\begin{bmatrix}0&0&-1&0\\0&0&0&-1\\1&0&0&0\\0&1&0&0\end{bmatrix},$$

$$\mathbf{A}_{q,4} = \begin{bmatrix} 0 & 0 & 0 & -1 \\ 0 & 0 & 1 & 0 \\ 0 & -1 & 0 & 0 \\ 1 & 0 & 0 & 0 \end{bmatrix}. \tag{42}$$

To efficiently prove it, let's define an intermediate intermediary matrix:

$$\bar{\mathbf{A}}_{p,q} := \mathbf{A}_p \mathbf{A}_q^H \in \mathrm{C}^{N_p L_p \times N_q L_q}, \tag{43}$$

where

$$\mathbf{A}_p := \left[\mathbf{A}_{p,1}^T \cdots \mathbf{A}_{p,L_p}^T\right]^T \in \mathrm{C}^{N_p L_p \times K}, \quad \mathbf{A}_q := \left[\mathbf{A}_{q,1}^T \cdots \mathbf{A}_{q,L_q}^T\right]^T \in \mathrm{C}^{N_q L_q \times K}. \tag{44}$$

It is noticed that the (i, j)th $N_p \times N_q$ block submatrix of $\bar{\mathbf{A}}_{p,q}$, for $i = 1, \ldots, L_p$ and $j = 1, \ldots, L_q$, is $\mathbf{A}_{p,i}\mathbf{A}_{q,j}^H$. In particular, for case (a), $\mathbf{A}_{p,i}$ and $\mathbf{A}_{q,j}$, for $i, j = 1, \ldots, 4$, is given in (40) and (42), respectively. It can be shown, after some manipulations, that

$$\bar{\mathbf{A}}_{p,q} = \begin{bmatrix} \mathbf{A}_{p,1} & -\mathbf{A}_{p,2} & \mathbf{A}_{p,3} & -\mathbf{A}_{p,4} \\ \mathbf{A}_{p,2} & \mathbf{A}_{p,1} & \mathbf{A}_{p,4} & \mathbf{A}_{p,3} \\ \mathbf{A}_{p,3} & -\mathbf{A}_{p,4} & -\mathbf{A}_{p,1} & -\mathbf{A}_{p,2} \\ \mathbf{A}_{p,4} & -\mathbf{A}_{p,3} & -\mathbf{A}_{p,2} & \mathbf{A}_{p,1} \end{bmatrix}. \tag{45}$$

Observing from (45), with $\mathbf{A}_{p,i}$ regarded as a particular variable, we can find that the matrix $\bar{\mathbf{A}}_{p,q}$ belongs to a (super) orthogonal design. With above discussions, we can conclude that the resultant structure of $\bar{\mathbf{A}}_{p,q}$ can be completely and directly observed from that of $\mathbf{F}_{p,q}$. This means that in order to examine the structure of $\mathbf{F}_{p,q}$ we only need to check the structure of $\bar{\mathbf{A}}_{p,q}$.

For $N_q = 3$, $\mathbf{A}_{q,j}$, $j = 1, \ldots, L_q$ can be easily obtained as that shown in (42) by deleting the last row of it. Also, it can be shown that $\bar{\mathbf{A}}_{p,q}$ has exactly the same structure as that given by (45). Similarly, for $i, j = 1, \ldots, 4$, we can also obtain $f_{q,q}^{(i,i)} = \alpha_q$ and $f_{q,q}^{(i,j)} = 0$ whenever $i \neq j$. Based on the above results, case (a) of Part (p3) is proved.

For case (b) of Part (p3), the results can be shown by identifying the matrix $\bar{\mathbf{A}}_{p,q}$ and following the same procedures described in (42–45), in which $\bar{\mathbf{A}}_{p,q}$ can be computed as follows:

$$\bar{\mathbf{A}}_{p,q} = \begin{bmatrix} \mathbf{A}_{p,1} & -\mathbf{A}_{p,2} & -\mathbf{A}_{p,3} & -\mathbf{A}_{p,4} \\ \mathbf{A}_{p,2} & \mathbf{A}_{p,1} & \mathbf{A}_{p,4} & -\mathbf{A}_{p,3} \\ \mathbf{A}_{p,3} & -\mathbf{A}_{p,4} & \mathbf{A}_{p,1} & \mathbf{A}_{p,2} \\ \mathbf{A}_{p,4} & \mathbf{A}_{p,3} & -\mathbf{A}_{p,2} & \mathbf{A}_{p,1} \end{bmatrix}. \tag{46}$$

□

B Proof of Lemma 4.1

Parts (p1) and (p4) of Lemma 4.1 have been shown in [24]. It only needs to prove Parts (p2–p3).

Proof of (p2) Noticed that for real-valued constellations, the distinct structure of $\mathbf{F}_{p,q}$ is completely and directly determined by that of $\bar{\mathbf{A}}_{p,q}$. However, in complex-valued constellations, the resultant structure of $\bar{\mathbf{A}}_{p,q}$ cannot directly and previously determine that of $\mathbf{F}_{p,q}$.

To effectively examine the structure of $\mathbf{F}_{p,q}$, let's define the following four basic matrices:

$$\mathcal{A}_1 := \begin{bmatrix} 1 & 0 \\ 0 & 1 \end{bmatrix}, \quad \mathcal{A}_2 := \begin{bmatrix} 0 & -1 \\ 1 & 0 \end{bmatrix}, \quad \mathcal{A}_3 := \begin{bmatrix} 1 & 0 \\ 0 & -1 \end{bmatrix}, \quad \mathcal{A}_4 := \begin{bmatrix} 0 & 1 \\ 1 & 0 \end{bmatrix}. \tag{47}$$

Also defining $\mathcal{A} := \left[\mathcal{A}_1^T \cdots \mathcal{A}_4^T\right]^T$, we obtain the fact:

$$\mathcal{A}\mathcal{A}^T = \begin{bmatrix} \mathcal{A}_1 & -\mathcal{A}_2 & \mathcal{A}_3 & \mathcal{A}_4 \\ \mathcal{A}_2 & \mathcal{A}_1 & \mathcal{A}_4 & -\mathcal{A}_3 \\ \mathcal{A}_3 & \mathcal{A}_4 & \mathcal{A}_1 & -\mathcal{A}_2 \\ \mathcal{A}_4 & -\mathcal{A}_3 & \mathcal{A}_2 & \mathcal{A}_1 \end{bmatrix}, \tag{48}$$

For $K = 8$, and $N_p = N_q = 2, k = l$, we have

$$\mathbf{A}_{p,k} = \mathbf{A}_{q,l} = \begin{cases} \mathbf{e}_{\lceil (k/2) \rceil}^T \otimes \mathcal{A}_1 & \text{if } k \text{ is odd} \\ \mathbf{e}_{\lceil (k/2) \rceil}^T \otimes \mathcal{A}_2 & \text{if } k \text{ is even} \end{cases} \quad k = 1, \ldots, 8,$$

$$\mathbf{A}_{p,k} = \mathbf{A}_{q,l} = \begin{cases} j \cdot \mathbf{e}_{\lceil (k-8)/2 \rceil}^T \otimes \mathcal{A}_3 & \text{if } k \text{ is odd} \\ j \cdot \mathbf{e}_{\lceil (k-8)/2 \rceil}^T \otimes \mathcal{A}_4 & \text{if } k \text{ is even} \end{cases} \quad k = 9, \ldots, 16, \tag{49}$$

where $\mathbf{e}_i$ is the ith unit standard vector in R^4. Based on (49) and using the fact (48) and the following properties:

$$(\mathbf{A} \otimes \mathbf{B})^H = \mathbf{A}^H \otimes \mathbf{B}^H, \qquad (\mathbf{A} \otimes \mathbf{B})(\mathbf{C} \otimes \mathbf{D}) = (\mathbf{AC} \otimes \mathbf{BD}), \tag{50}$$

it can be checked with (39) that each 2×2 block diagonal matrix of $\mathbf{F}_{p,q}^{(s,t)} \in \mathrm{R}^{8\times 8}, s, t = 1, 2$, belongs to an orthogonal design. Also, it can be observed that $\mathbf{F}_{p,q}^{(1,1)} = \mathbf{F}_{p,q}^{(2,2)}$ and $\mathbf{F}_{p,q}^{(1,2)} = -\mathbf{F}_{p,q}^{(2,1)}$. □

Proof of (p3) Similarly, to identify the structure of $\mathbf{F}_{p,q}$, let's define the following augmented matrices:

$$\mathcal{B}_1 := \mathcal{A}_1 \otimes \mathcal{A}_1, \qquad \mathcal{B}_2 := \mathcal{A}_3 \otimes \mathcal{A}_2, \qquad \mathcal{B}_3 := \mathcal{A}_2 \otimes \mathcal{A}_1, \qquad \mathcal{B}_4 := \mathcal{A}_4 \otimes \mathcal{A}_2, \tag{51}$$

where $\mathcal{A}_i, i = 1, \ldots, 4$, are defined in (47). For $N_q \in \{3, 4\}$, $\mathbf{A}_{q,l}$, can be determined as the direct augmentation of two $\mathcal{B}_i$ matrices, that is [13]

$$\mathbf{A}_{q,l} = \left[j^{\lfloor (l-1)/4 \rfloor} \mathcal{B}_{mod(l,4)} \ (-j)^{\lfloor (l-1)/4 \rfloor} \mathcal{B}_{mod(l,4)} \right], \quad l = 1, \ldots, 8, \tag{52}$$

where $mod(x, y)$ denotes the remainder after y dividing x, and $\mathcal{B}_0 := \mathcal{B}_4$. Based on (49) and (52), $\mathbf{A}_{p,i}\mathbf{A}_{q,j}^H$ ca be calculated and then substitute it into (39). Gathering each piece of $f_{p,q}^{(i,j)}$ and putting them altogether to determine $\mathbf{F}_{p,q}$, it can be shown that $\mathbf{F}_{p,q}$ indeed has the desired properties. □

C Proof of Theorem 4.1

To prove Theorem 4.1, some preliminary operation results of orthogonal matrix are examined. Let $K \in \{2, 4, 8\}$, it can be directly checked by analytic computations that, if both $\mathbf{Q}_1$ and $\mathbf{Q}_2$ lie in $\mathcal{O}(K)$, then so are $\mathbf{Q}_1 + \mathbf{Q}_2$ and $\mathbf{Q}_1 \cdot \mathbf{Q}_2$. The result can be precisely described as follows:

When the set $\mathcal{O}(K)$ is closed under addition and multiplication for any $\mathbf{Q}_1 \in \mathcal{O}(K)$, it is easy to observed that $\mathbf{Q}_1 + \mathbf{Q}_1^T = \gamma \mathbf{I}_K$ for some γ.

We will prove Theorem 4.1 by induction. When $G_i = 1$, the result is obvious since $\mathbf{F}_i = \alpha_{i,1}\mathbf{I}_{M_1}$, with $M_1 \in \{2, 4, 8\}$. Assume that the result is true for an arbitrary $G_i > 1$, i.e., $\mathbf{F}_i \in \tilde{\mathcal{F}}_{J_i}(G_i, D_i)$ implies $\mathbf{F}_i^{-1} \in \tilde{\mathcal{F}}_{J_i}(G_i)$ for such a G_i. It is required to check that $\mathbf{F}_{i-1}^{-1} \in \tilde{\mathcal{F}}_{J_{i-1}}(G_i + 1)$ (since $G_i + 1 = G_{i-1}$), whenever $\mathbf{F}_{i-1} \in \tilde{\mathcal{F}}_{J_{i-1}}(G_i + 1, D_{i-1})$. Let us partition an arbitrary $\mathbf{F}_{i-1} \in \tilde{\mathcal{F}}_{J_{i-1}}(G_i + 1, D_{i-1})$ as

$$\mathbf{F}_{i-1} := \begin{bmatrix} \mathbf{A} & \mathbf{B} \\ \mathbf{B}^T & \mathbf{D} \end{bmatrix} \in \mathrm{R}^{J_{i-1} \times J_{i-1}}, \tag{53}$$

where $\mathbf{A} \in \mathrm{R}^{J_i \times J_i}$, $\mathbf{B} \in \mathrm{R}^{J_i \times L_{\lceil \mathcal{I}_{i-1}(G_i+1)/2 \rceil}}$, and $\mathbf{D} \in \mathrm{R}^{L_{\lceil \mathcal{I}_{i-1}(G_i+1)/2 \rceil} \times L_{\lceil \mathcal{I}_{i-1}(G_i+1)/2 \rceil}}$. It is noteworthy that since $\mathbf{F}_{i-1} \in \tilde{\mathcal{F}}_{J_{i-1}}(G_i + 1, D_{i-1})$, (a) $\mathbf{A} \in \tilde{\mathcal{F}}_{J_i}(G_i, D_i)$ and hence $\mathbf{A}^{-1} \in \tilde{\mathcal{F}}_{J_i}(G_i)$ by assumption (b) if we write $\mathbf{B} := \left[\mathbf{B}_1^T \ldots \mathbf{B}_{G_i}^T\right]^T$, where $\mathbf{B}_l \in \mathrm{R}^{L_{\lceil \mathcal{I}_i(l)/2 \rceil} \times L_{\lceil \mathcal{I}_{i-1}(G_i+1)/2 \rceil}}$, $l = 1, \ldots, G_i$, whose matrix structure has been established in Lemma 4.1 (or Table 4) (c) $\mathbf{D} = c\mathbf{I}_{L_{\lceil \mathcal{I}_{i-1}(G_i+1)/2 \rceil}}$. Also, $\mathbf{F}_i^{-1}$ can be similarly written as

$$\mathbf{F}_i^{-1} := \begin{bmatrix} \bar{\mathbf{A}} & \bar{\mathbf{B}} \\ \bar{\mathbf{B}}^T & \bar{\mathbf{D}} \end{bmatrix} \in \mathrm{R}^{J_{i-1} \times J_{i-1}}, \tag{54}$$

where $\bar{\mathbf{A}} \in \mathrm{R}^{J_i \times J_i}$, $\bar{\mathbf{B}} \in \mathrm{R}^{J_i \times L_{\lceil \mathcal{I}_{i-1}(G_i+1)/2 \rceil}}$, and $\bar{\mathbf{D}} \in \mathrm{R}^{L_{\lceil \mathcal{I}_{i-1}(G_i+1)/2 \rceil} \times L_{\lceil \mathcal{I}_{i-1}(G_i+1)/2 \rceil}}$. To show that $\mathbf{F}_{i-1}^{-1} \in \tilde{\mathcal{F}}_{J_{i-1}}(G_i + 1)$, it suffices to check that (i) $\bar{\mathbf{A}} \in \tilde{\mathcal{F}}_{J_i}(G_i)$ (ii) Define $\bar{\mathbf{B}} := \left[\bar{\mathbf{B}}_1^T \ldots \bar{\mathbf{B}}_{G_i}^T\right]^T$, where $\bar{\mathbf{B}}_l \in \mathrm{R}^{L_{\lceil \mathcal{I}_i(l)/2 \rceil} \times L_{\lceil \mathcal{I}_{i-1}(G_i+1)/2 \rceil}}$, $l = 1, \ldots, G_i$, each 4×4 block off-diagonal submatrix of $\bar{\mathbf{B}}_l$ belongs to $\mathcal{O}(4)$ or is a zero matrix $\mathbf{O}_4$ (iii) $\bar{\mathbf{D}} = d\mathbf{I}_{L_{\lceil \mathcal{I}_{i-1}(G_i+1)/2 \rceil}}$. Properties (i–iii) can be shown based on the inversion formula for block matrices:

$$\mathbf{F}_i^{-1} = \begin{bmatrix} \bar{\mathbf{A}} & \bar{\mathbf{B}} \\ \bar{\mathbf{B}}^T & \bar{\mathbf{D}} \end{bmatrix} = \begin{bmatrix} \left(\mathbf{A} - \mathbf{B}\mathbf{D}^{-1}\mathbf{B}^T\right)^{-1} & -\left(\mathbf{A} - \mathbf{B}\mathbf{D}^{-1}\mathbf{B}^T\right)^{-1}\mathbf{B}\mathbf{D}^{-1} \\ -\left(\mathbf{D} - \mathbf{B}^T\mathbf{A}^{-1}\mathbf{B}\right)^{-1}\mathbf{B}^T\mathbf{A}^{-1} & \left(\mathbf{D} - \mathbf{B}^T\mathbf{A}^{-1}\mathbf{B}\right)^{-1} \end{bmatrix}. \tag{55}$$

Proof of (i) From (55), $\bar{\mathbf{A}} = \left(\mathbf{A} - \mathbf{B}\mathbf{D}^{-1}\mathbf{B}^T\right)^{-1} = \left(\mathbf{A} - \frac{1}{c}\mathbf{B}\mathbf{B}^T\right)^{-1}$. Since $\mathbf{A} \in \tilde{\mathcal{F}}_{J_i}(G_i, D_i)$, to prove $\bar{\mathbf{A}} \in \tilde{\mathcal{F}}_{J_i}(G_i)$, it suffices to check the structure of $\mathbf{B}\mathbf{B}^T$. In particular, $\mathbf{B}\mathbf{B}^T$ can be expressed as follows:

$$\mathbf{B}\mathbf{B}^T = \begin{bmatrix} \mathbf{B}_1 \\ \vdots \\ \mathbf{B}_{G_i} \end{bmatrix} \left[\mathbf{B}_1^T \cdots \mathbf{B}_{G_i}^T\right] = \begin{bmatrix} \mathbf{B}_1\mathbf{B}_1^T & \cdots & \mathbf{B}_1\mathbf{B}_{G_i}^T \\ \vdots & \ddots & \vdots \\ \mathbf{B}_{G_i}\mathbf{B}_1^T & \cdots & \mathbf{B}_{G_i}\mathbf{B}_{G_i}^T \end{bmatrix}, \tag{56}$$

where $\mathbf{B}_k\mathbf{B}_l^T$, $k, l, = 1, \ldots, G_i$, has the following structures. (a) If $N_{\lceil \mathcal{I}_i(l)/2 \rceil} = N_{\lceil \mathcal{I}_{i-1}(G_i+1)/2 \rceil} = 2$, then according to (p2) of Lemma 4.1 $\mathbf{B}_l \in \mathcal{O}(8, 2)$ or $\mathbf{B}_l = \mathbf{O}_8$. Therefore, $\mathbf{B}_l\mathbf{B}_l^T = c_l\mathbf{I}_8$ or $\mathbf{B}_l\mathbf{B}_l^T = \mathbf{O}_8$. (b) If $N_{\lceil \mathcal{I}_i(l)/2 \rceil} = 3$ or 4, $N_{\lceil \mathcal{I}_{i-1}(G_i+1)/2 \rceil} = 2$, then according to (p3) of Lemma 4.1 each 4×4 submatrix of $\mathbf{B}_l \in \mathrm{R}^{4\times 8}$ belongs to an orthogonal design. It can be easily checked that $\mathbf{B}_l\mathbf{B}_l^T = c_l\mathbf{I}_4$. (c) If $N_{\lceil \mathcal{I}_i(l)/2 \rceil} = 2$, $N_{\lceil \mathcal{I}_{i-1}(G_i+1)/2 \rceil} = 3$ or 4, then according to (p3) of lemma 4.1 each 4×4 submatrix of $\mathbf{B}_l \in \mathrm{R}^{8\times 4}$ belongs to an orthogonal design. It can be verified that

$$\mathbf{B}_l\mathbf{B}_l^T = \begin{bmatrix} c_l\mathbf{I}_4 & -c_l\mathbf{I}_4 \\ -c_l\mathbf{I}_4 & c_l\mathbf{I}_4 \end{bmatrix}. \tag{57}$$

(d) If $N_{\lceil \mathcal{I}_i(l)/2 \rceil} = N_{\lceil \mathcal{I}_{i-1}(G_i+1)/2 \rceil} = 3$ or 4, then according to (p4) of Lemma 4.1 $\mathbf{B}_l \in \mathcal{O}(4)$ or $\mathbf{B}_l = \mathbf{O}_4$, $\mathbf{B}_l\mathbf{B}_l^T = c_l\mathbf{I}_4$ or $\mathbf{B}_l\mathbf{B}_l^T = \mathbf{O}_4$. Based on the results (a–d), it can be observed that the diagonal entries of $\mathbf{B}_l\mathbf{B}_l^T$ are the same. (e) To check the structure of $\mathbf{B}_k\mathbf{B}_l^T$, whenever $k \neq l$, it should be firstly identified the families of $\mathbf{B}_k$'s and $\mathbf{B}_l$'s according to Lemma 4.1, and then compute $\mathbf{B}_k\mathbf{B}_l^T$. Using the same procedures as done in (a–d) above, it can be observed that each 4×4 block submatrix of $\mathbf{B}_k\mathbf{B}_l^T$ belongs to an orthogonal design, or is a scaled identity matrix or zero matrix. Based on above results, $\mathbf{B}\mathbf{B}^T \in \tilde{\mathcal{F}}_{J_i}(G_i', D_i')$, where $G_i' = G_i$ and $D_i \leq D_i' \leq G_i$. This leads to $\left(\mathbf{A} - \frac{1}{c}\mathbf{B}\mathbf{B}^T\right) \in \tilde{\mathcal{F}}_{J_i}(G_i', D_i')$ since $\mathbf{A} \subset \mathbf{B}\mathbf{B}^T$. As a result, it can be obtained $\bar{\mathbf{A}} = \left(\mathbf{A} - \frac{1}{c}\mathbf{B}\mathbf{B}^T\right)^{-1} \in \tilde{\mathcal{F}}_{J_i}(G_i')$ by assumption. This proves property (i). □

Proof of (ii) From (55), $\bar{\mathbf{B}} = -\bar{\mathbf{A}}\mathbf{B}\mathbf{D}^{-1} = \frac{1}{c}\bar{\mathbf{A}}\mathbf{B}$, and it suffices to check the structure of $\bar{\mathbf{A}}\mathbf{B}$. From the proof of (i), it can be observed that each 4×4 block submatrix of $\bar{\mathbf{A}}$ or $\mathbf{B}$ belongs to an orthogonal design or is a zero matrix. By using the results of Lemma 4.1 and operation results of the orthogonal matrix, it can be verified that each 4×4 block submatrix of $\bar{\mathbf{A}}\mathbf{B}$ will also belong to an orthogonal design or be a zero matrix, which follows property (ii). □

Proof of (iii) Since $\bar{\mathbf{D}} = \left(\mathbf{D} - \mathbf{B}^T\mathbf{A}^{-1}\mathbf{B}\right)^{-1}$ and $\mathbf{D} = c\mathbf{I}_{L_{\lceil \mathcal{I}_{i-1}(G_i+1)/2 \rceil}}$, to prove property (iii), it suffices to check that $\mathbf{B}^T\mathbf{A}^{-1}\mathbf{B}$ is a scalar multiple of $\mathbf{I}_{L_{\lceil \mathcal{I}_{i-1}(G_i+1)/2 \rceil}}$. Eventually, for $k, l = 1, \ldots, G_i$, denote $\mathbf{U}_{k,l}$ be the (k,l)th $L_{\lceil \mathcal{I}_{i-1}(k)/2 \rceil} \times L_{\lceil \mathcal{I}_{i-1}(l)/2 \rceil}$ block submatrix of $\mathbf{A}^{-1}$. Since $\mathbf{B} = \left[\mathbf{B}_1^T \cdots \mathbf{B}_{G_i}^T\right]^T$, it is easy to check that

$$\begin{aligned}\mathbf{B}^T\mathbf{A}^{-1}\mathbf{B} &= \sum_{k,l=1}^{G_i} \mathbf{B}_k^T\mathbf{U}_{k,l}\mathbf{B}_l \\ &= \sum_{k=1}^{L} \mathbf{B}_k^T\mathbf{U}_{k,k}\mathbf{B}_k + \sum_{k,l=1,k\neq l}^{G_i} \mathbf{B}_k^T\mathbf{U}_{k,l}\mathbf{B}_l. \end{aligned} \tag{58}$$

Since $\mathbf{A}^{-1} \in \tilde{\mathcal{F}}_{J_i}(G_i), \mathbf{U}_{k,k} = \eta_k\mathbf{I}_{L_{\lceil \mathcal{I}_{i-1}(k)/2 \rceil}}$ for some scalar η_k. By using the operation results of orthogonal matrix, the first summation on the right-hand-side of the second equality in (58) can be reformulated as

$$\begin{aligned}\sum_{k=1}^{G_i} \mathbf{B}_k^T\mathbf{U}_{k,k}\mathbf{B}_k &= \sum_{k=1}^{G_i} \eta_k\mathbf{B}_k^T\mathbf{B}_k \\ &= \begin{cases} \alpha_k\mathbf{I}_{L_{\lceil \mathcal{I}_{i-1}(G_i+1)/2 \rceil}} & \text{if } N_{\lceil \mathcal{I}_i(k)/2 \rceil}, N_{\lceil \mathcal{I}_{i-1}(G_i+1)/2 \rceil} = 2, \\ a_k\mathbf{I}_4 & \text{if } N_{\lceil \mathcal{I}_i(k)/2 \rceil} = 2, N_{\lceil \mathcal{I}_{i-1}(G_i+1)/2 \rceil} \in \{3,4\}. \end{cases} \end{aligned} \tag{59}$$

On the other hand, since $k, l = 1, \ldots, G_i$, each 4×4 block submatrix of $\mathbf{U}_{k,l}$ or $\mathbf{B}_k$ belongs to an orthogonal design or is a zero matrix by assumption, then each 4×4 block submatrix of $\mathbf{B}_k^T\mathbf{U}_{k,l}\mathbf{B}_l$ also belongs to an orthogonal design or is a zero matrix. Therefore, by using the operation results of orthogonal matrix, it follows that:

$$\begin{aligned}&\mathbf{B}_k^T\mathbf{U}_{k,l}\mathbf{B}_l + \mathbf{B}_l^T\mathbf{U}_{l,k}\mathbf{B}_k \\ &\quad= \begin{cases} \mu_k\mathbf{I}_{L_{\lceil \mathcal{I}_{i-1}(G_i+1)/2 \rceil}} & \text{if } N_{\lceil \mathcal{I}_i(k)/2 \rceil}, N_{\lceil \mathcal{I}_{i-1}(G_i+1)/2 \rceil} = 2, \\ \delta_k\mathbf{I}_4 & \text{if } N_{\lceil \mathcal{I}_i(k)/2 \rceil} = 2, N_{\lceil \mathcal{I}_{i-1}(G_i+1)/2 \rceil} \in \{3,4\}. \end{cases} \end{aligned} \tag{60}$$

From (60), it can be verified that

$$\sum_{k,l=1,k\neq l}^{L} \mathbf{B}_k^T \mathbf{U}_{k,l} \mathbf{B}_l = \begin{cases} \beta_k \mathbf{I}_{L_{\lceil \mathcal{I}_{i-1}(G_i+1)/2 \rceil}} & \text{if } N_{\lceil \mathcal{I}_i(k)/2 \rceil}, N_{\lceil \mathcal{I}_{i-1}(G_i+1)/2 \rceil} = 2, \\ b_k \mathbf{I}_4 & \text{if } N_{\lceil \mathcal{I}_i(k)/2 \rceil} = 2, N_{\lceil \mathcal{I}_{i-1}(G_i+1)/2 \rceil} \in \{3,4\}. \end{cases} \quad (61)$$

Theorem 4.1 thus asserts. □

References

1. 3GPP TR 25.814. (2006). Physical layer aspects for evolved UTRA (Release 7). Release 7, v. 7.0.0.
2. IEEE 802.16e Std. (2006). IEEE standard for local and metropolitan area networks Part 16: Air interface for fixed and mobile broadband wireless access systems amendment 2: Physical and medium access control layers for combined fixed and mobile operation in licensed bands and corrigendum 1. IEEE Std 802.16e-2005 and IEEE Std 802.16-2004/Cor 1-2005.
3. Gesbert, D., Shafi, M., Shiu, D., Smith, P. J., & Naguib, A. (2003). From theory to practice: An overview of MIMO space-time coded wireless systems. *IEEE Journal of Select on Areas in Communication, 21*(3), 281–302.
4. Paulraj, A. J., Gore, D. A., Nabar, R. U., & Bölcskei, H. (2004). An overview of MIMO communications—A key to gigabit wireless. *Proceedings of the IEEE, 92*(2), 198–218.
5. Diggavi, S. N., Al-Dhahir, N., Stamoulis, A., & Calderbank, A. R. (2004). An great expectations: The value of spatial diversity in wireless networks. *Proceedings of the IEEE, 92*(2), 219–270.
6. Paulraj, A. J., & Papadias, C. B. (1997). Space-time processing for wireless communications. *IEEE Signal Processing Magazine, 14*(11), 49–83.
7. Paulraj, A. J., Nabar, R., & Gore, D. (2003). *Introduction to space-time wireless communications*. Cambridge University Press.
8. Foschini, G. J. (1996). Layered space-time architecture for wireless communication in a fading environment when using multi-element antennas. *Bell Laboratories Technical Journal., 1*, 45–49.
9. Foschini, G. J., & Gans, M. J. (1998). On limits of wireless communications in a fading environment when using multiple antennas. *Wireless Personal Communications, 6*(3), 311–335.
10. Golden, G. D., Foschini, G. J., Valenzuela, R. A., & Wolniansky, P. W. (1999). Detection algorithm and initial laboratory results using V-BLAST space-time communication structure. *Electronic Letters, 35*(1), 14–16.
11. Tarokh, V., Seshadri, N., & Calderbank, A. R. (1998). Space-time codes for high data rate wireless communication: Performance criterion and code construction. *IEEE Transactions on Information Theory, 44*(2), 744–765.
12. Alamouti, S. (1998). A simple transmit diversity scheme for wireless communications. *IEEE Journal on Selected Areas in Communications, 16*(8), 1451–1458.
13. Tarokh, V., Jafarkhani, H., & Calderbank, A. R. (1999). Space-time block codes from orthogonal designs. *IEEE Transactions on Information Theory, 45*(7), 1456–1467.
14. Larsson, E. G., & Stoica, P. (2003). *Space-time block coding for wireless communications*. Cambridge University Press.
15. Zheng, L., & Tse, D. N. C. (2003). Diversity and multiplexing: A fundamental tradeoff in multiple-antenna channels. *IEEE Transactions on Information Theory, 49*(5), 1073–1096.
16. Proakis, J. G. (2001). *Digital communications*, (4th edn.). The McGraw-Hill Companies, Inc.
17. Gesbert, D., Haumonte, L., Bolcskei, H., Krishnamoorthy, R., & Paulraj, A. J. (2002). Technologies and performance for non-line-of-sight broadband wireless access network. *IEEE Communications Magazine, 40*(4), 86–95.
18. Kim, I. M., & Tarokh, V. (2001). Variable-rate space-time block codes in M-ary PSK systems. *IEEE Journal on Selected Areas in Communications, 21*(3), 362–373.
19. Naguib, A. F., Seshadri, N., & Calderbank, A. R. (1998). Applications of space-time block codes and interference suppression for high capacity and high data rate wireless systems. *Proceedings of the IEEE 32th Asilomar Conference on Signals, Systems, and Computers*, Vol. 2, pp. 1803–1810, Nov. 1998.
20. Stamoulis, A., Al-Dhahir, N., & Calderbank, A. R. (2001). Further results on interference cancellation and space-time block codes. *Proceedings of the IEEE 35th Asilomar Conference on Signals, Systems, and Computers*, Vol. 1, Nov. 2001, pp. 257–261.
21. Tarokh, V., Naguib, A., Seshadri, N., & Calderbank, A. R. (1999). Combined array processing and space-time coding. *IEEE Transactions an Information Theory, 45*(4), 1121–1128.

22. Tao, M., & Chen, R. S. (2004). Generalized layered space-time codes for high data rate wireless communications. *IEEE Transactions on Wireless Communications, 3*(4), 1067–1075.
23. Dai, Y., Lei, Z., & Sun, S. (2004). Ordered array processing for space-time coded systems. *IEEE Communications Letters, 8*(8), 526–528.
24. Ho, C. L., Wu, J. Y., & Lee, T. S. (2004). Block-based symbol detection for high rate space-time coded systems. *Proceedings of the IEEE VTC 2004-Spring*, Vol. 1, May 2004, pp. 375–379.
25. Ho, C. L., Wu, J. Y., & Lee, T. S. (2006). Group-wise V-BLAST detection in multiuser space-time dual-signaling wireless systems. *IEEE Transactions an Wireless Communications, 5*(7), 1896–1909
26. Wu, J. Y., Ho, C. L., & Lee, T. S. (2006). Detection of multiuser orthogonal space-time block coded signal via ordered successive interference cancellation. *IEEE Transactions an Wireless Communications, 5*(7), 1594–1600.
27. Catreux, S., Gesbert, D., & Heath, R. W. (2002). Adaptive modulation and MIMO coding for broadband wireless data networks. *IEEE Communications Magazine, 40*(6), 108–115.
28. Chung, S. T., & Goldsmith, A. J. (2001). Degree of freedom in adaptive modulation: A unified view. *IEEE Transactions an Communications, 49*(9), 1561–1571.
29. Tirkkonen, O., Boariu, A., & Hottinen, A. (2002). Minimum ono-orthogonality rate 1 space-time block code for 3+ Tx. *IEEE ISSSTA 2002*, pp. 429–432.

Author Biographies

Chung-Lien Ho was born in Taoyuan Taiwan, R.O.C., in June 1974. He received the B.S. degree in the Department of Electrical Engineering from Da Yeh University, Changhua, Taiwan, R.O.C., in 1996, the M.S. degree in the Department of Electrical and Computer Science Engineering from Yuan Ze University, Taoyuan, Taiwan, R.O.C., in 1998, and the Ph.D. degree in the Department of Communication Engineering from National Chiao Tung University, Hsinchu, Taiwan, R.O.C., in 2005. His current research interests include the spacetime signal processing, multiple-input multiple-output signal processing for wireless communications and statistical signal processing.

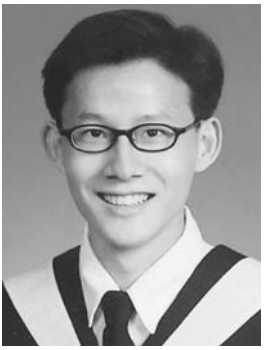

Fan-Shuo Tseng was born in Kaushiung, Taiwan, in 1980. He received the B.S. degree in Electrical Engineering from the Fu-Jen Catholic University, Taiwan, in 2002, and the M.S. degree in Communication Engineering from the National Central University, Taiwan, in 2004. He is currently working toward the Ph.D. degree in the Department of Communication Engineering at the National Chiao Tung University. His current areas of interest research include space-time signal processing for wireless communications and statistical signal processing.

Ta-Sung Lee received the B.S. degree from National Taiwan University in 1983, the M.S. degree from the University of Wisconsin, Madison, in 1987, and Ph.D. degree from Purdue University, W. Lafayette, IN, in 1989, all in electrical engineering. In 1990, he joined the Faculty of National Chiao Tung University (NCTU), Hsinchu, Taiwan, where he now holds a position as Professor of Department of Communication Engineering and Dean of Student Affairs of NCTU. During 2005-2007, he was Chairman of Department of Communication Engineering. His other current positions include Director of IEEE Taipei Section, Vice Chair of IEEE COMSOC Taipei Chapter, Technical Advisor at Information & Communications Research Labs. of Industrial Technology Research Institute (ITRI), Taiwan. He is active in research and development in advanced techniques for wireless communications, such as smart antenna and MIMO technologies, cross-layer design, and SDR prototyping of advanced communication systems. He has co-led several National Research Programs, such as "Program for Promoting Academic Excellence of Universities – Phases I & II" and "MoE Aiming for the Top University (ATU) Program". Dr. Lee has won several awards for his research, engineering and teaching contributions; these include two times National Science Council (NSC) superior research award, Young Electrical Engineer Award of the Chinese Institute of Electrical Engineers, and NCTU Teaching Award.